Available online at www.sciencedirect.com
ScienceDirect
Tectonophysics 426 (2006) 335–360
TECTONOPHYSICS
www.elsevier.com/locate/tecto

Late orogenic, large-scale rotations in the Tien Shan and adjacent mobile belts in Kyrgyzstan and Kazakhstan

Rob Van der Voo [a,*], Natalia M. Levashova [b], Ludmila I. Skrinnik [c], Taras V. Kara [b,d], Mikhail L. Bazhenov [b,a]

[a] Department of Geological Sciences, University of Michigan, Ann Arbor, Michigan 48109-1005, USA
[b] Geological Institute, Academy of Sciences of Russia, Pyzhevsky Lane, 7, Moscow, 109017, Russia
[c] Institute of Geological Sciences, Kabanbay Batyr, 69a, 480010, Almaty, Republic of Kazakhstan
[d] Geological Faculty, Moscow State University, Leninskye Gory, Moscow, 119899, Russia

Received 28 April 2006; received in revised form 12 August 2006; accepted 21 August 2006
Available online 25 September 2006

Abstract

Most of Kazakhstan belongs to the central part of the Eurasian Paleozoic mobile belts for which previously proposed tectonic scenarios have been rather disparate. Of particular interest is the origin of strongly curved Middle and Late Paleozoic volcanic belts of island-arc and Andean-arc affinities that dominate the structure of Kazakhstan. We undertook a paleomagnetic study of Carboniferous to Upper Permian volcanics and sediments from several localities in the Ili River basin between the Tien Shan and the Junggar–Alatau ranges in southeast Kazakhstan. Our main goal was to investigate the Permian kinematic evolution of these belts, particularly in terms of rotations about vertical axes, in the hope of deciphering the dynamics that played a role during the latest Paleozoic deformation in this area. This deformation, in turn, can then be related to the amalgamation of this area with Baltica, Siberia, and Tarim in the expanding Eurasian supercontinent. Thermal demagnetization revealed that most Permian rocks retained a pretilting and likely primary component, which is of reversed polarity at three localities and normal at the fourth. In contrast, most Carboniferous rocks are dominated by postfolding reversed overprints of probably "mid-Permian" age, whereas presumably primary components are isolated from a few sites at two localities. Mean inclinations of primary components generally agree with coeval reference values extrapolated from Baltica, whereas declinations from primary as well as secondary components are deflected counterclockwise (ccw) by up to ~90°. Such ccw rotated directions have previously also been observed in other Tien Shan sampling areas and in the adjacent Tarim Block to the south. However, two other areas in Kazakhstan show clockwise (cw) rotations of Permian magnetization directions. One area is located in the Kendyktas block about 300 km to the west of the Ili River valley, and the other is found in the Chingiz Range, to the north of Lake Balkhash and about 400 km to the north of the Ili River valley. The timing of the ccw as well as cw rotations is clearly later than the disappearance of any marine basins from northern Tarim, the Tien Shan and eastern Kazakhstan, so that the rotations cannot be attributed to island-arc or Andean-margin plate settings — instead we attribute the rotations to large-scale, east–west (present-day coordinates), sinistral wrenching in an intracontinental setting, related to convergence between Siberia and Baltica, as recently proposed by Natal'in and Şengör [Natal'in, B.A., and Şengör, A.M.C., 2005. Late Palaeozoic to Triassic evolution of the Turan and Scythian platforms: the pre-history of the palaeo-Tethyan closure, Tectonophysics, 404, 175–202.]. Our previous work in the Chingiz and North Tien Shan areas on Ordovician and Silurian rocks suggested relative rotations of ~180°, whereas the Permian declination differences are of the order of 90° between the two areas. Thus, we assume that about 50% of the total post-Ordovician rotations are of pre-Late Permian age,

* Corresponding author. Tel.: +1 734 764 8322; fax: +1 734 763 4690.
E-mail addresses: voo@umich.edu (R. Van der Voo), mibazh@mail.ru (N.M. Levashova), lisgeo@inbox.ru (L.I. Skrinnik).

0040-1951/$ - see front matter
doi:10.1016/j.tecto.2006.08.008

with the other half of Late Permian–earliest Mesozoic age. The pre-Late Permian rotations are likely related to oroclinal bending during plate boundary evolution in a supra-subduction setting, given the calc-alkaline character of nearly all of the pre-Late Permian volcanics in the strongly curved belts.

Keywords: Altaids; Paleomagnetism; Rotations; Wrench-faulting; Permian

1. Introduction to the regional tectonic issues

Eurasia is comprised of several major blocks with Precambrian basement separated by multiple mobile belts with different Phanerozoic ages (Fig. 1A). As such, it is the only presently existing supercontinent and represents a superb natural laboratory for elucidating and testing ideas about the formation of past supercontinents like Gondwana or Rodinia. Paleomagnetic data can help to decipher paleolatitudinal motion and/or internal deformation of cratons, microcontinents, and the mobile zones between them, provided that the spatial and temporal density of the results is sufficiently high. Because of the paucity of reliable paleomagnetic data, the evolution of the Paleozoic belts in Kazakhstan is still enigmatic. Moreover, while it is generally accepted that the formation of Central Asia's crust is the consequence of collisions between the European (i.e., Baltica), Siberian, Tarim and North China cratons (Fig. 1A), models for its internal deformation remain controversial (compare Didenko et al., 1994; Şengör and Natal'in, 1996; Filippova et al., 2001). Large-scale deformation within the belt, particularly in the wide triangular area between Siberia, Tarim and Baltica that includes Kazakhstan and the North Tien Shan, has clearly occurred in order to produce the highly fragmented and contorted structures. The scarcity of paleomagnetic data allows some authors to assume a relative rigidity of some large fragments within the belt (e.g., Filippova et al., 2001), whereas major large-scale and intense deformation that "crumpled" a 6000-km long island-arc, called the Kipchak Arc, has been hypothesized by other researchers (Şengör and Natal'in, 1996; see also Natal'in and Şengör, 2005).

Kazakhstan is likely one of the more complex parts of the Paleozoic mobile belts in Central Asia. Its Early Paleozoic to Silurian structure includes numerous fragments of subduction-related magmatic arcs, accretionary wedges, flysch basins, and Precambrian microcontinents with Early Paleozoic siliciclastic-carbonate cover (see Şengör and Natal'in, 1996). These units often form T-like and Y-like junctions, and no prevailing structural trends can be identified. The Middle–Late Paleozoic pattern of Kazakhstan is dominated by strongly curved subduction-related magmatic arcs (Fig. 1B), which unconformably overlie older structures. The external belt comprises volcano-sedimentary Silurian rocks and a thick Lower–Middle Devonian terrestrial volcanic pile, which is likely to have marked an Andean-type convergent margin (Filippova et al., 2001). In the Frasnian, volcanic activity shifted about 150 km to the south and southeast in the northern part of the area and continued there in the Famennian–Tournaisian (not shown separately). Further inward shifts of volcanic activity to the Junggar–Balkhash Basin occurred in the Early Carboniferous and lasted until the mid-Permian. Late Permian (and locally Early Triassic) volcanism is confined to several smaller basins that are spread along the older volcanic belt and is no longer of island-arc affinity. The lateral shift of volcanism is negligible in the southern arms of the volcanic belts, is noticeable in their northern arms, and is the largest in the central hinge zones (Fig. 1B). This volcanic activity lasted for about 150 Ma, while terrigenous sedimentation continued in the inner parts of the loop-like belts. As a result, the Late Devonian–Early Carboniferous volcanics overlie the Silurian and Early Devonian flysch series and accretionary wedges.

All volcanic belts contain rhyolite, andesite–dacite and andesite–basalt complexes. The composition of the volcanic series strongly varies within each belt, but everywhere progresses from basalt to andesite and dacite and then to rhyolite (Tectonics of Kazakhstan, 1982). Since the Silurian and until the Late Early Permian, the volcanics are of calc-alkaline affinity and are considered to be related to outward subduction from a shrinking ocean basin that was located in the present-day interior of the arcs (Kurchavov, 2001; Tevelev, 2001). Several deformation events affected these belts, but, generally, the volcanics are not strongly deformed, except for limited areas close to large faults.

Taken at face value, the petrological data would imply that a three-sided subduction zone, dipping below an active semi-circular continental margin, surrounded a basin with gradually vanishing oceanic crust. Surprisingly, this zone would then have slowly propagated

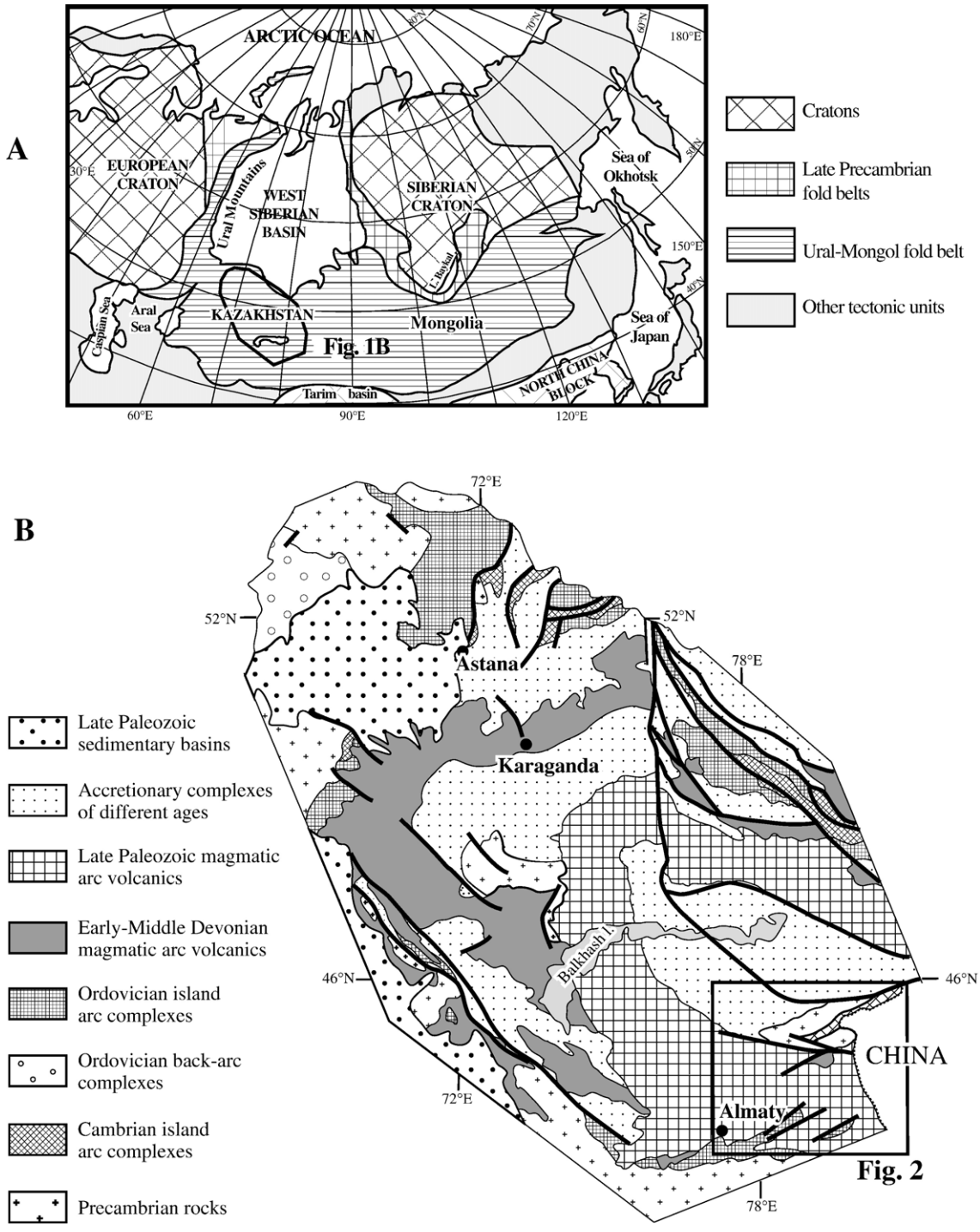

Fig. 1. (A) Location of the Ural–Mongol fold belt within Eurasia and outline of Fig. 1B in Kazakhstan. (B) Schematic map of major rock complexes in Kazakhstan, simplified after Degtyarev (2003) with main faults shown as thick solid lines.

inward, preserving its horseshoe-shaped form, while a steadily shrinking oceanic basin existed for about 150 Ma until its complete extinction. Such a configuration, however, is hardly imaginable within the plate tectonic concept and has no analogues in the present-day world. Still, some authors regard the curvatures of the volcanic belts as primary features (Zaytsev, 1984; Kurchavov, 2001), while others advocate oroclinal

bending but disagree on its timing (Zonenshain et al., 1990; Şengör and Natal'in, 1996; Tevelev, 2001; Skrinnik, 2003). Taking into account the large dimensions of these volcanic structures, as well as the tectonic evolution of the entire Ural–Mongol belt, changes in the relative paleogeographic positions of Baltica, Siberia and Tarim must have strongly influenced their origin. Up to now, convincing geological evidence for the evolution of the regional structures is lacking, whereas pre-Permian paleomagnetic data for some areas are in need of substantiation (e.g., Grishin et al., 1997; Burtman et al., 1998a,b) or are still rather scarce for other areas (Bazhenov et al., 2003; Collins et al., 2003; Levashova et al., 2003b; Alexyutin et al., 2005a,b).

There are several Ordovician–Silurian paleomagnetic results published thus far, which come either from the North Tien Shan in the southern limb of the curved structures of Fig. 1B (Bazhenov et al., 2003; Alexyutin et al., 2005a,b), or from their northern limb in the Chingiz Range (Collins et al., 2003; Levashova et al., 2003b). If we assume that normal polarity directions are represented by shallowly upward Late Ordovician inclinations for both sampling regions, then the declinations are on average, some 180° apart. This led Levashova and colleagues (2003b) to interpret the curved structures as secondary, i.e., as having been subjected to oroclinal bending (Van der Voo, 2004). The assumption that the magnetic directions identified in the southern limb of the horseshoe-shaped structure are of normal polarity has recently been supported by paleomagnetic data from Middle Paleozoic rocks (Levashova et al., 2005). However, this polarity choice also needs further substantiation for the northern limb, either by confirmation from similarly rotated directions from younger rocks, or by documentation of consistent rotation patterns not just in the limbs, but also in the hinge zones of the curved belts. In order to test whether younger rocks from the two regions show a coherent rotational pattern, we collected Carboniferous and Permian rocks from the southern arm of the Balkhash–Ili Zone in southeastern Kazakhstan, where no paleomagnetic data had thus far become available (Figs. 1B and 2). In the northern region (Chingiz Range), Permian paleomagnetic results are already available (Levashova et al., 2003a,b; Collins et al., 2003). The declinations obtained in the present study will be compared with those expected for the area if it would have been rigidly attached to Baltica or Siberia, as well as with those from the Chingiz Range. Declination deviations will be taken as indications of rotations about vertical axes, and can then be analyzed in the context of Central Asian tectonic deformation models for Late Paleozoic–earliest Mesozoic time.

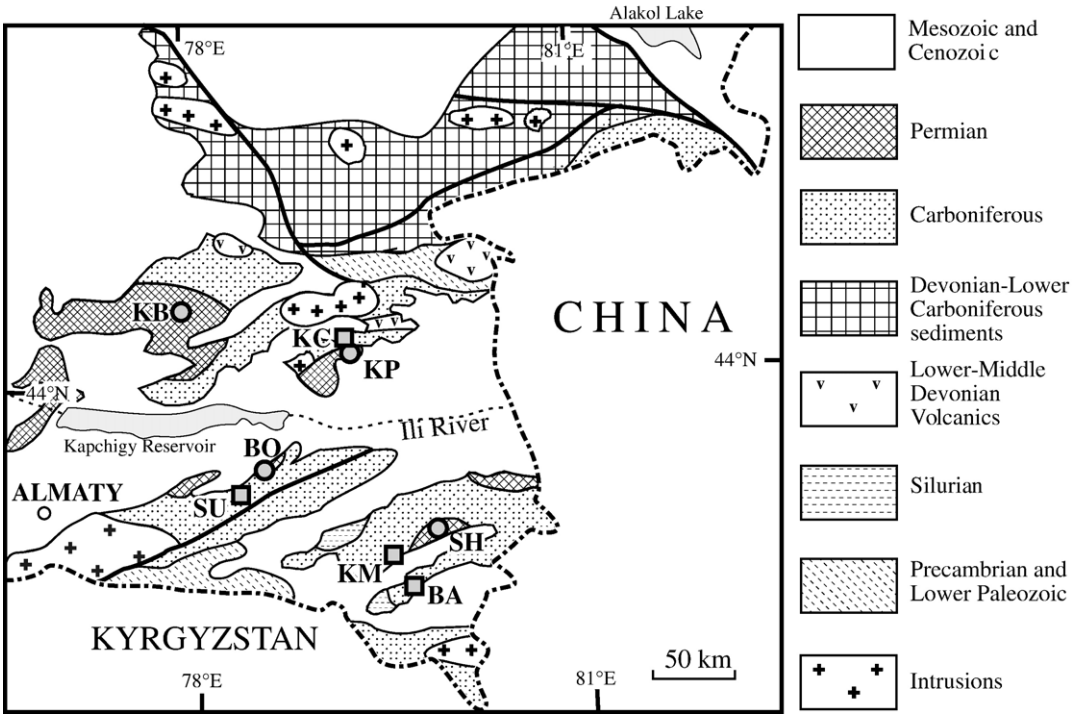

Fig. 2. Geological map of the sampling area in southeast Kazakhstan. Thick solid lines denote major faults. Sampling localities of four Upper Permian and four Carboniferous formations are labeled as in the text and are shown as circles and squares, respectively.

2. Local geological setting and sampling

The study area is located in the Ili River valley area between the Tien Shan to the south and the Junggar–Alatau Range in the north (Fig. 2). In China, these two ranges converge and become there the branches of the Tien Shan Mountains *sensu lato*. The oldest rocks in this area are Precambrian granites and gneisses overlain by Neoproterozoic to Cambrian carbonates and carbon-rich slates, which in turn are unconformably covered by Ordovician volcanic and sedimentary rocks. These rocks were deformed and intruded by granites at the end of the Ordovician. After the Early Devonian, SE Kazakhstan continued to be an area of active volcanism, with some interruptions, until the Late Permian and, locally, the Early Triassic (Skrinnik and Grishina, 1997; Skrinnik et al., 1998; Bekzhanov et al., 2000). Continental sedimentary deposits of Jurassic and/or younger age overlie the Paleozoic volcanics with a major angular unconformity.

In our study area, Early Carboniferous volcanic rocks rest with a weak angular unconformity on Devonian rocks and with a major unconformity on older complexes. Regional deformation took place in the Middle Pennsylvanian (Moscovian stage), whereas in our study area younger, Late Pennsylvanian to Permian, rocks form gentle monoclines and broad open folds that developed during the latest Permian–Early Triassic (elsewhere, Permian strata are more strongly deformed). At the same time, several angular unconformities, locally up to 20°, are known within the Late Paleozoic volcanic sequence (Skrinnik, 1989). Partly, this could be due to the mode of emplacement of these mostly subaerial volcanic rocks that erupted from different sources and could have accumulated on tilted surfaces, but some tilting can also be related to post-eruption local subsidence. Alpine deformation resulted in the formation of gentle, regional tilts (~10°), although steep monoclines and tight folds are found close to faults active in the Neogene.

Southeastern Kazakhstan is regarded as a part of an Early Paleozoic tectonic zone that can be traced further northwest into central and north Kazakhstan (Apollonov, 2000; Bekzhanov et al., 2000). In terms of the curved mid-Late Paleozoic volcanic belts of Fig. 1B, the study area belongs to the southern arm.

Four Carboniferous and four Permian targets were sampled (Fig. 2). Brief descriptions below follow the two-letter abbreviations used to identify the sampling areas (see labels in Fig. 2).

KM: at this locality (43°05'N, 79°39'E), we collected Tournaisian (Lower Carboniferous) gray to violet-gray tuffaceous sandstones and siltstones, with a conglomerate layer at the top (site KM-C). These strata are conformably overlain by black basalt flows with thin interbeds of red tuffaceous sediments. Closer to the section base, the sediments are intruded by gabbroic bodies, which are compositionally close to the basalts and are thought to be coeval feeding conduits that cooled quickly close to the surface. We sampled seven sites (KM1-7) from sediments, seven sites (KM8-14) from basalt flows, and 22 lava cobbles from the conglomerate member (KM-C).

BA: here (42°52'N, 79°45'E), four sites were sampled from Tournaisian tuffaceous red sandstone about 60 m thick.

SU: at this locality (43°27'N, 78°38'E), we collected Tournaisian rocks from two monoclinal sections about two kilometers apart. At the first one, the pile of basalts is some 300 m thick. Six sites (SU1–6) were taken from the upper 150 m only, because no reliable stratification could be found in the lower half. In addition, seven volcanic bombs and two lava cobbles were sampled from within a layer of coarse-grained tuff at the section top, in order to apply the conglomerate test (site SU-C). Only two sites (SU7-8) of brown-red tuffs could be taken from the second section.

KC: at locality KC (44°16'N, 79°28'E) to the north of the Ili River, samples were collected from a ~700 m thick, southward-dipping, monoclinal section of Pennsylvanian, most likely Bashkirian, interbedded gray, green and red gritstones, sandstones, siltstones, and medium to acid tuffs. A total of six KC-sites were sampled exclusively from finer-grained lithologies.

SH, KB: at localities SH (43°10'N, 79°52'E) and KB (44°24'N, 78°00'E), Upper Permian basalt flows with thin red interbeds were studied.

KP: samples are from three sites in Upper Permian redbeds at this locality (44°14'N, 79°29'E), plus one basaltic site and one site from dacitic tuff at the section top and base, respectively.

BO: dacitic and acid tuffs, tuffaceous sandstone and siltstones, and two andesite–basalt flows were sampled at locality BO (43°33'N, 78°37'E). This and all other Upper Permian localities are found in monoclines; dip azimuths and dip angles are listed in Table 1 for the Permian collections.

All sampled formations accumulated above the sea level, and their ages are based on flora and pollen (Skrinnik and Grishina, 1997; Skrinnik et al., 1998; Bekzhanov et al., 2000). In lava sections, each site consists either of a single flow, or of two adjacent flows. If individual lava flows could not be recognized at an exposure, a site can consist of a section up to ~10 m thick. A site in sedimentary sections may consist of 5–15 m of strata. From each site, we took between five and

Table 1
Mean directions in Upper Permian rocks from the North Tien Shan and the Junggar–Alatau ranges

S/L	*N*	B	In situ				Tilt-corrected			
			D°	I°	*k*	α_{95}°	D°	I°	*k*	α_{95}°
ChRM										
BO1	6/6	303/27	162.5	−64.1	156	5.4	144.4	−40.1	147	5.5
BO2	7/6	302/33	171.1	−64.3	224	4.5	146.1	−37.4	152	5.4
BO3	6/6	303/32	162.0	−63.3	103	6.6	143.2	−35.1	99	6.8
BO4	6/6	302/44	208.2	−65.8	47	9.8	154.3	−39.9	54	9.2
BO5	8/8	307/45	221.4	−67.5	125	5.0	158.1	−42.4	125	5.0
BO6	8/8	307/45	230.4	−64.3	204	3.9	163.7	−45.1	204	3.9
BO7	6/6	307/44	215.5	−68.4	115	6.3	156.7	−41.4	75	7.8
BO	(7/7)		194.7	−67.9	44	9.2	152.1	−40.4	142	5.1
ChRM										
SH1	7/6	169/28	210.3	−3.0	58	8.9	214.4	−22.1	64	8.5
SH2	6/6	174/26	210.6	−13.9	102	6.7	218.2	−34.1	68	6.8
SH3	6/6	171/27	192.0	−21.1	65	8.4	199.7	−46.0	62	8.5
SH4	8/7	173/27	198.2	−22.6	30	11.2	207.7	−46.4	29	11.5
SH5	6/5	173/27	188.5	−25.4	103	7.6	195.5	−51.1	103	7.6
SH	(5/5)		200.2	−17.4	37	12.7	208.2	−40.3	35	13.2
ITC										
KP-I[a]	31/5		149.3	−30.6	54	10.5	167.8	−63.7	238	5.0
HTC										
KP1	6/6	169/28	152.4	−24.1	35	11.5	145.0	−50.3	38	10.9
KP2	5/5	138/33	158.2	−21.2	43	11.8	169.2	−51.3	41	12.0
KP3	5/2	142/36	153.0	−9.9	37	12.8	157.5	−44.9	48	11.1
KP4	8/8	143/42	147.3	−12.1	63	7.0	150.3	−53.5	57	7.0
KP5	7/7	143/42	156.2	−11.9	82	6.7	164.1	−52.1	83	6.7
KP-H	(5/5)		153.4	−15.9	116	7.1	157.2	−50.8	133	6.7
ITC										
KB3	6/4	224/19	183.6	−44.8	90	10.3	177.1	−63.4	61	12.5
KB4	7/4	172/23	155.6	−39.6	118	8.5	145.9	−61.3	130	8.1
KB6	8/8	166.20	179.3	−45.0	169	4.5	183.6	−63.5	136	5.0
KB7	8/4	171/20	173.8	−47.2	45	14.6	181.3	−68.0	44	14.7
KB-I	(8/4)		172.8	−44.7	72	10.9	171.3	−64.9	95	9.5
HTC and ChRM										
KB1	5/5	162/20	335.5	35.6	62	9.8	332.5	55.8	58	10.1
KB2	7/6	161/22	329.2	35.7	743	2.6	323.4	56.7	525	3.1
KB3[b]	6/5	224/19	355.2	41.3	8	32.5	338.3	51.5	13	25.0
KB4	7/6	172/23	324.1	25.7	166	5.6	315.1	45.3	189	5.2
KB5	7/6	170/24	322.6	30.6	35	11.9	311.2	50.7	35	12.0
KB6	8/7	166/20	328.3	23.2	90	6.7	323.9	42.3	87	6.8
KB7	8/8	171/20	318.5	35.2	23	12.0	306.6	51.0	25	11.6
KB8	10/9	168/29	333.3	21.3	22	11.4	327.2	48.7	22	11.4
KB-H	(8/7)		330.4	31.5	49	8.0	322.0	50.7	95	5.7
TR[c]	(13/5)		167.3	−42.3	37	12.6	170.6	−64.6	125	6.9
PER	(24/24)		–	34.9	7	11.0	–	45.4	53	3.8

Explanations: S/L, sites/localities labeled as in the text and Fig. 1B; locality symbols followed by -I or -H correspond to locality-means for ITC or HTC (ChRM), respectively; TR, overprint of likely Early Triassic age in Upper Permian rocks from locality KB and KC of the Junggar Range; PER, primary component in Upper Permian rocks obtained with the aid of inclination-only statistics (McFadden and Reid, 1982); *N*, number of samples studied/accepted (if for sites, the ratio *N* is placed in parentheses); *B*, azimuth of dip/dip angle; D, declination; I, inclination; *k*, concentration parameter (Fisher, 1953); α_{95}, radius of 95% confidence circle.

[a] All samples from this locality combined.

[b] Excluded because of low precision.

[c] For ITC site-mean directions from locality KB and ITC locality-mean KP.

ten hand samples, oriented with a magnetic compass, or alternatively we drilled a similar number of cores oriented with a magnetic or solar compass. At most localities, a sufficient number of sedimentary units were found to obtain bedding attitudes for each site. Nevertheless, stratified rocks were scarce at localities SU, SH, and in the upper basaltic part of locality KM, where basalt flows prevail; for these collections, bedding measurements had to be extrapolated over up to 30 m of the true thickness in one or the other direction.

3. Methods

The collection was studied in the paleomagnetic laboratories of the Geological Institute of the Russian Academy of Sciences in Moscow and of the University of Michigan in Ann Arbor. In Moscow, cubic specimens of 8 cm^3 volume were cut from hand samples. Specimens were stepwise demagnetized in 15–20 increments up to 685 °C in a homemade oven with internal residual fields of about 10nT and measured with a JR-4 spinner magnetometer with a noise level of 0.1 mAm^{-1}. In Ann Arbor, cylindrical specimens of dimensions 2.2 cm × 2.5 cm as well as some cubes were stepwise demagnetized over a range of 50 °C–680 °C utilizing an Analytical Services TD-48 thermal demagnetizer; magnetizations were measured with a 2G Enterprises cryogenic magnetometer in a magnetically shielded room. No systematic difference was found between the samples that were treated in Moscow or Ann Arbor, and the data have been pooled.

Demagnetization results were plotted on orthogonal vector diagrams (Zijderveld, 1967). Visually identified linear trajectories were used to determine directions of magnetic components by Principal Component Analysis (PCA), employing a least-squares fit comprising three or more demagnetization steps (Kirschvink, 1980), anchoring the fitted lines to the origin where appropriate. The notation of paleomagnetic components, used in the description of results, is as follows. (1) A low-temperature component, LTC, is a remanence removed during the initial stage of demagnetization, usually below 300 °C. (2) A characteristic remanent magnetization, ChRM, is a remanence showing a rectilinear decay to the origin over the entire temperature range after removal of the LTC, if present. (3) An intermediate-temperature component, ITC, is a remanence that does not show rectilinear decay to the origin and is generally followed by a high-temperature component in the same sample or other samples in a given site. (4) A high-temperature component, HTC, is a remanence that shows rectilinear decay to the origin and is isolated after removal of an ITC. The HTC-label, then, in our scheme requires the presence of an ITC. An HTC direction may well be a result that is characteristic of a given site, but the ChRM-label is reserved for samples without an ITC, for reasons of clarity and consistency.

Site-mean directions were computed either using only the PCA-calculated sample directions or combining the latter with remagnetization circles employing the technique of McFadden and McElhinny (1988); great-circle trajectories included at least four steps. Paleomagnetic software written by Jean-Pascal Cogné (Cogné, 2003), Stanislav V. Shipunov and Randy Enkin (see URL http://gsc.nrcan.gc.ca/dir/index_e.php?id=12377) was used in the analysis.

4. Results

The LTC directions, which were isolated in thermal demagnetization below at most 300 °C from multiple samples from many localities, are either nearly random or cluster around the present-day field before tilt correction. This remanence is thus either a sum of spurious components acquired during transportation and laboratory treatment, or a viscous overprint. As this remanence carries no useful information, it is not further discussed below, and the NRM values are not shown on demagnetization diagrams.

4.1. Upper Permian rocks

After heating to 200–300°, a well-defined ChRM was isolated from most samples of lava and tuff from three of the four Permian localities (BO, SH and KP; Fig. 3A–D). The ChRM resides in both magnetite and hematite in varying proportions, but its directions do not depend on magnetic mineralogy (Fig. 3A–B). Such a pattern is likely to be due to high-temperature oxidation during emplacement of volcanic units, indicating a primary nature of the magnetizations. Redbeds from locality KP gave noisier data, but the presence of a similar component is evident there as well (Fig. 3E). In just five samples from locality KP, an ITC was removed between 300 °C and 580 °C (Fig. 3F; Table 1); as these samples came from different sites, the ITC locality-mean was calculated at the sample level. All components isolated at these three localities are reversed.

Some basalt flows from the fourth locality (KB) reveal only a ChRM (Fig. 3G), whereas in other flows both ITC and HTC are recognized (Fig. 3H). One of the flows with two magnetic components is intruded by a thin felsic sill in which only a reversed component appears to be present, below the highest demagnetization step at 690 °C (Fig. 3I). The age of this sill is unknown, but it is compositionally close to Lower

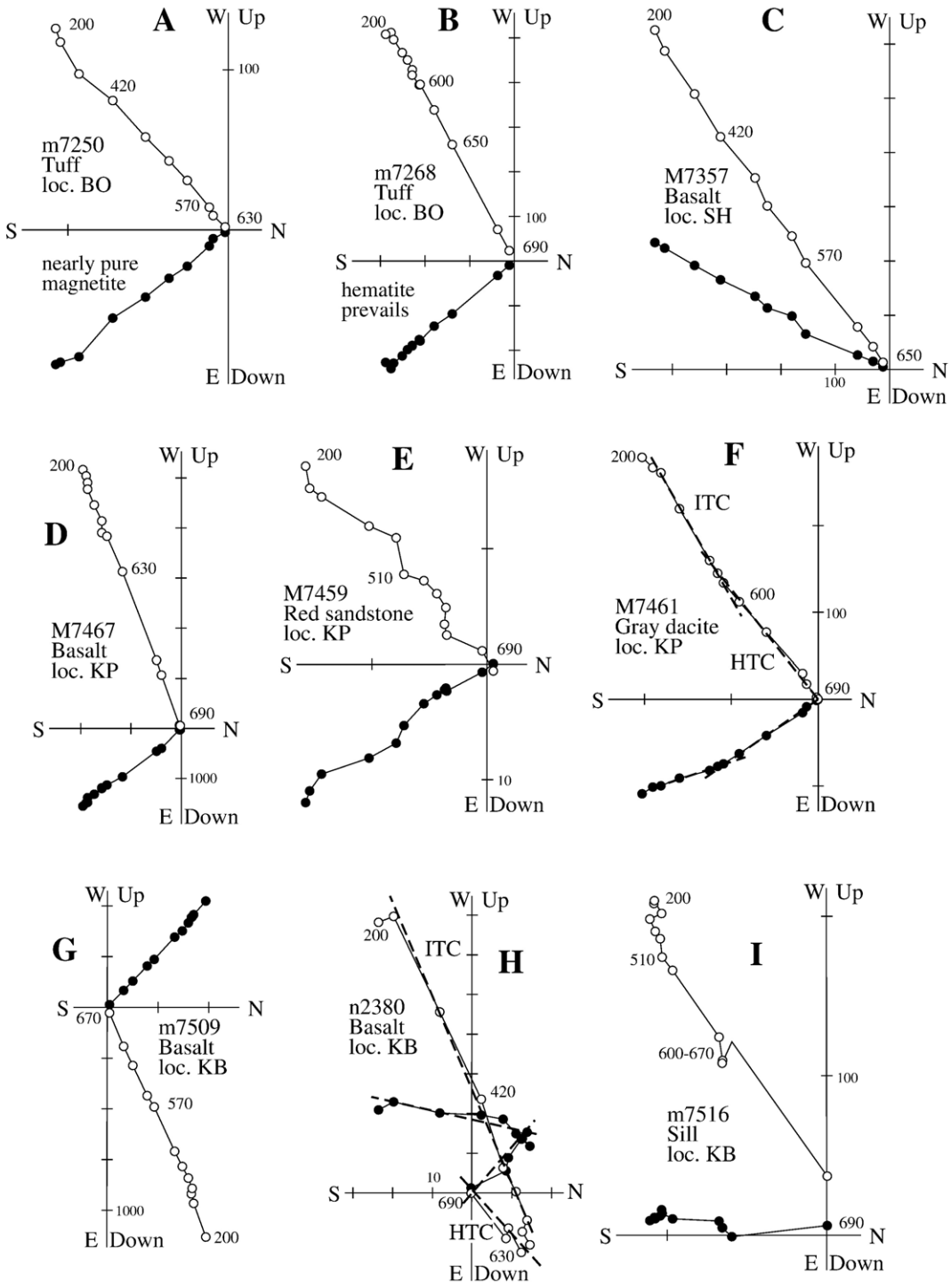

Fig. 3. Representative thermal demagnetization plots of Upper Permian rocks (with localities labeled as in text and tables and Fig. 2) in stratigraphic coordinates. Dashed lines marking paleomagnetic components in F and H are labeled as explained in the text; these lines are not shown in the plots for single component samples. Full (open) dots represent vector endpoints projected onto the horizontal (vertical) plane. Temperature steps are in degrees Celsius. Magnetization intensities are in mA/m. For clarity, NRM points are omitted from the plots.

Triassic acid lavas in the same area (Malaysary Fm., see Bekzhanov et al., 2000). We therefore assume that the reversed ITC in the basalt flows and the ChRM in this sill are approximately coeval. All HTC and ChRM directions in basalt samples from this locality have normal polarity, which confirms a post-Kiaman age; it is the only normal polarity observed in Upper Permian rocks in Kazakhstan and the western Tien Shan so far. We argue that the basalts at locality KB are somewhat younger than those at the other Upper Permian localities; even so, they belong to the same Late Permian andesite–basalt sequence as found in the other parts of southeast Kazakhstan (Bekzhanov et al., 2000).

Site-mean ChRM and HTC directions from localities BO, KB, and KP are plotted in Fig. 4C and D. Despite the approximately monoclinal nature of the strata at these localities, with only minor variations in bedding attitudes (see Table 1), the site-mean directions show their best grouping in stratigraphic coordinates upon incremental unfolding. We must note, however, that the study area suffered some Late Permian–Triassic as well as Cenozoic ("Alpine") tectonic instabilities, so that the (minor) variations in bedding attitudes that were used for the tilt test at each of the localities do not well constrain magnetization ages. Regardless, one can also consider the results from localities BO, KB and KP in the aggregate, and a tilt test on the combined site-mean directions (compare Fig. 4C and D for triangles, open circles and full diamonds) is convincingly positive.

For the uniformly dipping lava flows at locality SH, the tilt test is inconclusive (k changes from 37 to 35 upon untilting). Three of the SH site-means reach the same inclination values as those from the other three localities, whereas two inclination results seem to lag behind upon untilting. Judging from the demagnetization data (Fig. 3C), a Permian remanence is reliably isolated at locality SH, and the deviating (more

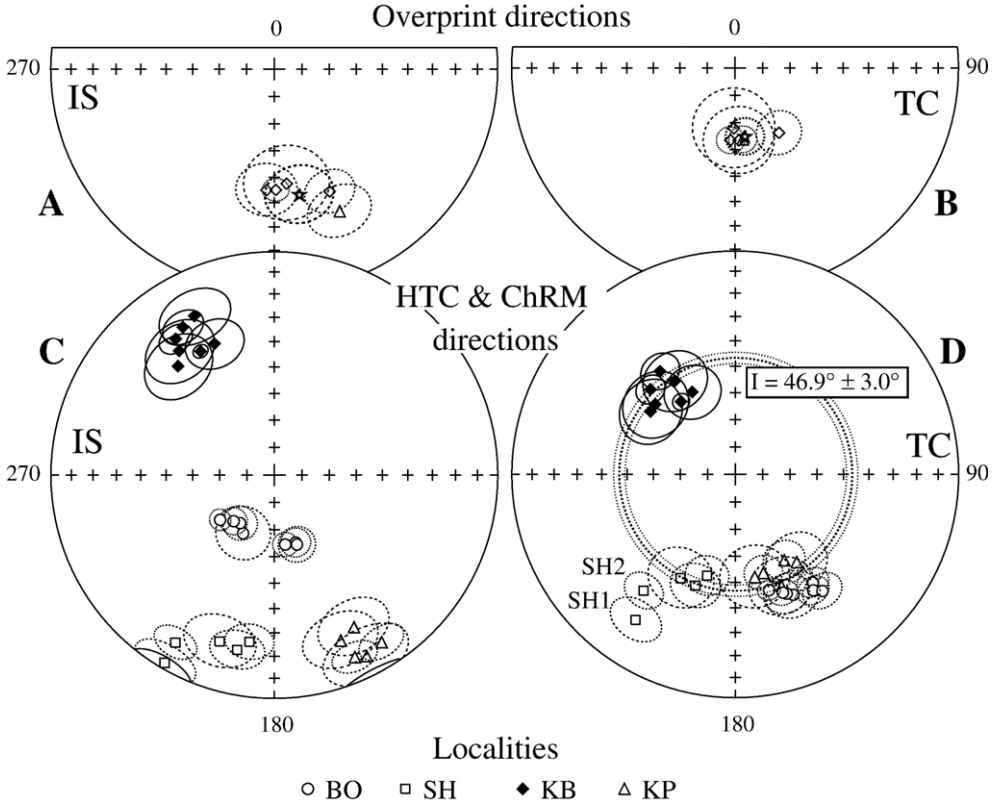

Fig. 4. Stereoplots of site-mean directions with associated confidence circles (thin lines) of the Upper Permian formations from southeast Kazakhstan in geographic (IS = in situ) and stratigraphic (TC = tilt-corrected) coordinates. Thick and thin dotted lines in (D) denote mean inclination and its confidence limits, respectively, computed with the aid of inclination-only statistics (McFadden and Reid, 1982). Solid (open) symbols and solid (dashed) lines are projected onto the lower (upper) hemisphere. HTC = high-temperature components, identified in samples where intermediate-temperature components (ITC, or overprint directions) are first removed; ChRM = characteristic remanent magnetization directions for samples where there is only one magnetic component after removal of a low-temperature component (LTC).

shallowly inclined) site-means (open squares, SH1 and SH2 in Fig. 4C–D) from this area are unlikely to be due to remagnetization. We think that the deviating (more shallow) SH directions result from minor tilt plus vertical-axis rotations as will be discussed below.

4.2. Carboniferous rocks

At locality KM (Fig. 5A), tuffaceous sediments from sites KM3–7 reveal a single component that persists up to 520° to 580° and sometimes decays to the origin (Fig. 5B)

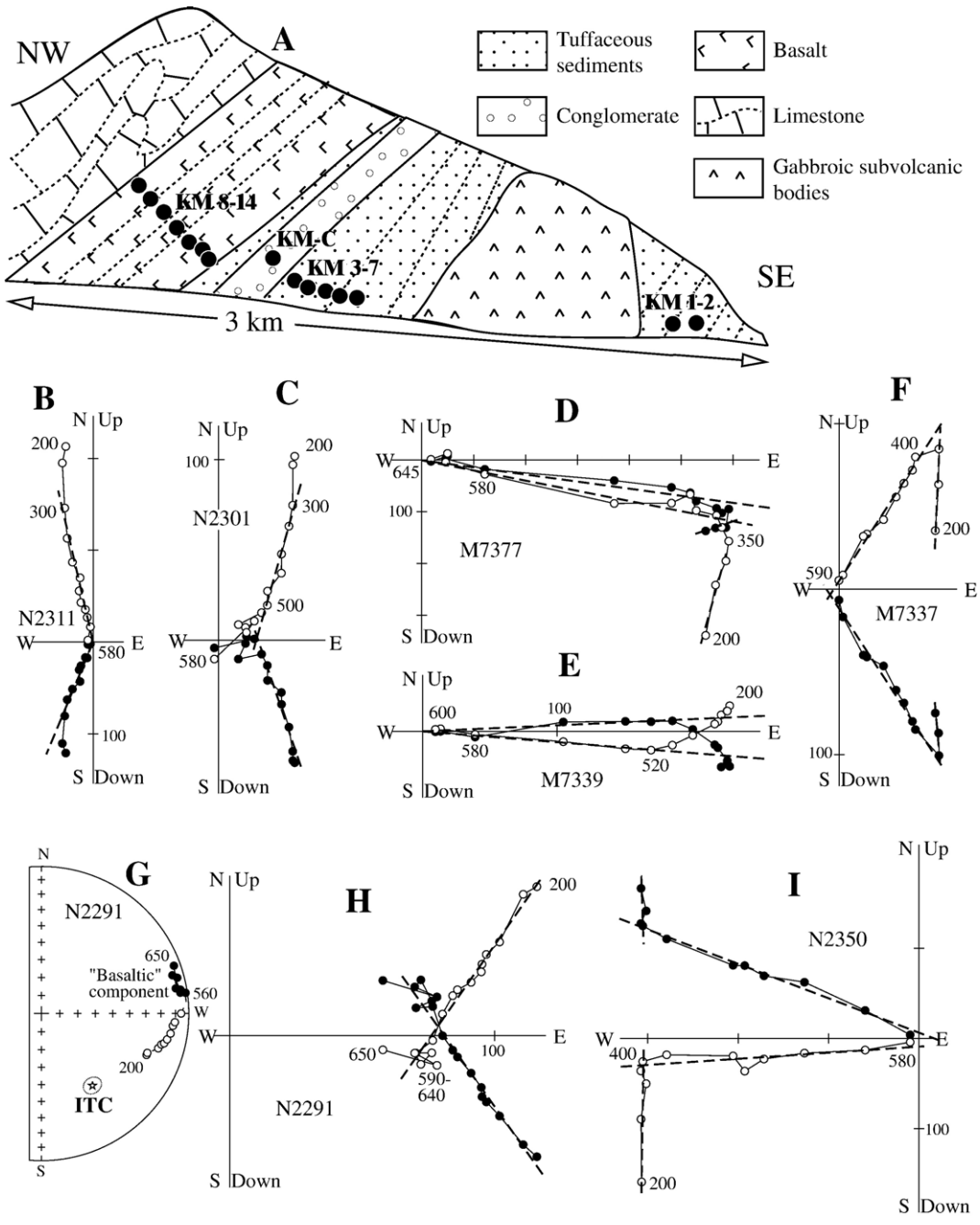

Fig. 5. (A) Schematic cross-section of locality KM, of Tournaisian (Lower Mississippian) age. Thin dotted lines indicate stratification; full dots represent sampling sites as labeled. (B–I) Results from locality KM, including representative thermal demagnetization plots (B–F, H–I) and a stereoplot (G) all in geographic (in situ) coordinates. Other explanations as in Figs. 3 and 4.

but usually misses it (Fig. 5C). This ITC is likely an overprint. Proper identification of an HTC at these sites is prevented by acquisition of spurious components (Fig. 5C), even though it is clear from diagrams such as that in Fig. 5C that an HTC exists.

In basalt flows (sites KM8–14), a LTC is omnipresent and often strong, but no ITC is observed. The high-temperature component must therefore (using our definition) be called a ChRM. This ChRM does not show consistent high-temperature directions in the samples with very strong LTC, whereas a nearly horizontal east-pointing ChRM could be isolated from those samples that have a lower-intensity LTC (Fig. 5D). The fact that we found no traces of the reversed ITC so prevalent in the tuffaceous sediments, and the correlation between magnetization intensity and directional behavior, indicate that this collection of basaltic sites is problematic.

In the sedimentary sites KM1 and KM2, which are close to the gabbroic intrusion (Fig. 5A), some samples reveal only the shallow-inclination, easterly "basaltic" component (Fig. 5E), while a remanence similar to the

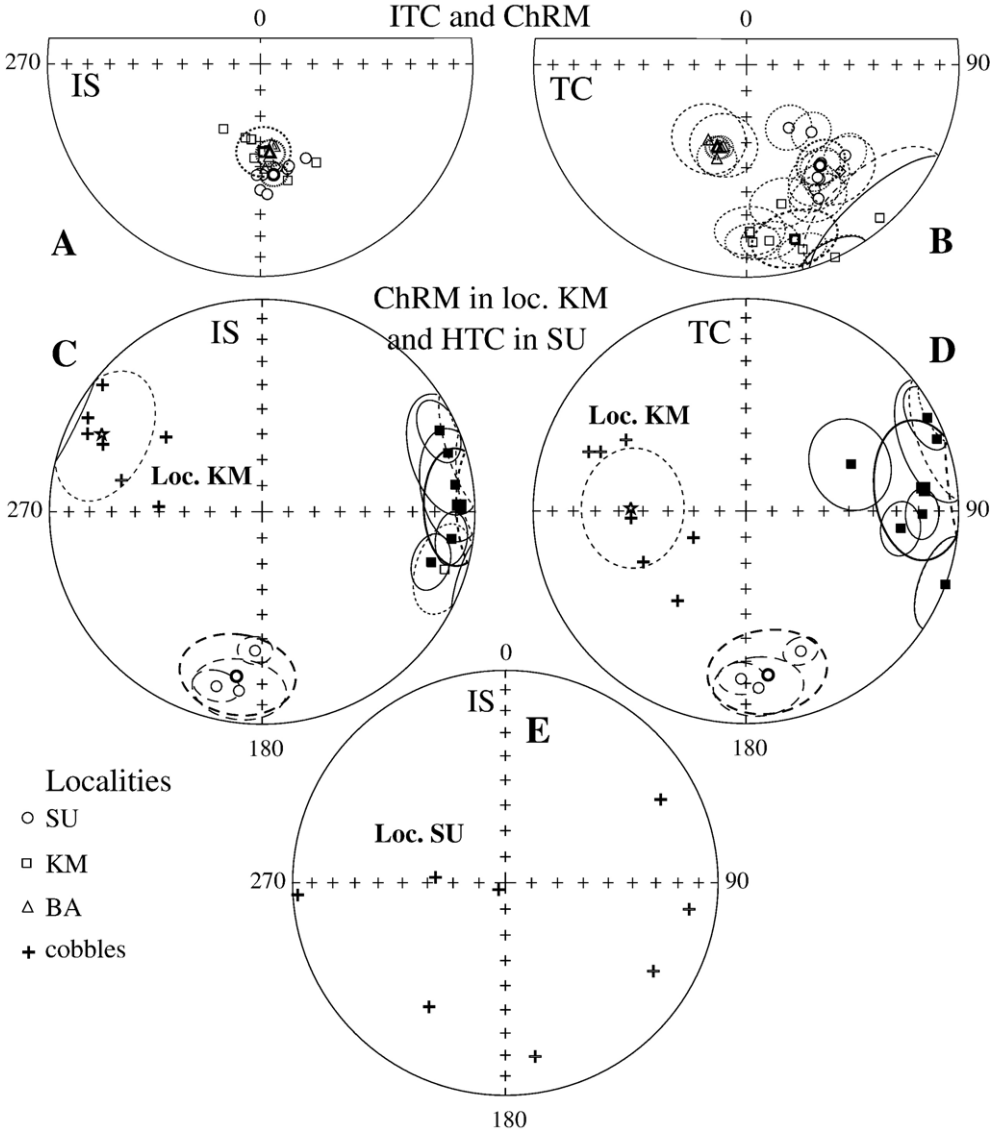

Fig. 6. Stereoplots of paleomagnetic directions with associated confidence circles (thin lines) from the Tournaisian rocks at localities SU, KM, and BA in the North Tien Shan. Larger symbols with thicker oval lines denote locality-mean directions with associated confidence circles. Crosses are ChRM directions from cobbles in conglomerates at localities KM (C–D) and SU (E); star is the ChRM cobble-mean direction with associated confidence circle for locality KM. Other explanations as in Fig. 4.

Table 2
Mean directions in Tournaisian (Lower Carboniferous) rocks from the North Tien Shan

S/L	*N*	B	In situ				Tilt-corrected			
			D°	I°	*k*	α_{95}°	D°	I°	*k*	α_{95}°
ITC										
KM1	6/3	295/46	150.4	−45.7	27	24.1	139.0	−5.0	27	24.1
KM2	9/7	308/50	166.8	−43.1	52	8.4	155.3	−0.3	43	9.3
KM3	10/9	329/48	174.2	−56.5	78	5.9	163.0	−10.2	51	7.3
KM4	7/7	333/54	209.5	−61.3	91	6.4	178.0	−17.7	52	8.5
KM5	6/6	318/35	191.4	−61.0	288	4.0	165.8	−33.0	40	10.8
KM6	5/5	338/35	186.7	−60.7	96	7.9	172.6	−17.6	77	8.8
KM7	3/3	350/32	183.5	−53.4	86	13.4	178.8	−22.4	122	11.2
KM-I	(14/7)		177.9	−55.8	38	9.9	164.4	−15.5	22	13.3
HTC and ChRM[a]										
KM1	6/5	295/46	82.2	8.9	22	16.6	66.0	44.8	22	16.6
KM2[b]	9/4	300/41	72.2	−5.8	10	40.7	67.6	21.6	12	37.5
KM8	9/6	350/29	72.7	8.8	15	18.1	69.4	4.2	15	18.1
KM9	7/7	350/29	98.2	10.5	62	7.8	90.9	18.0	61	7.8
KM10	8/8	350/26	106.7	17.6	40	8.9	96.5	27.4	40	8.9
KM11	10/9	8/30	107.7	−10.5	16	13.7	110.3	0.1	16	13.4
KM13	6/6	344/25	65.7	9.0	51	9.6	62.7	4.5	51	9.6
KM-H	(14/6)		88.8	7.7	17	16.9	83.1	17.1	10	21.7
KM-C	23/7	333/46	295.9	−17.4	9	21.3	271.4	−45.1	9	21.3
ITC and ChRM[a]										
SU1	9/7	266/37	180.0	−40.4	92	6.3	151.3	−33.6	43	9.3
SU2	6/5	270/36	180.4	−47.2	48	11.2	147.3	−36.5	49	11.0
SU3	8/3	268/37	176.9	−38.6	156	9.9	151.7	−29.3	156	9.9
SU4	9/9	268/37	181.8	−46.6	87	5.6	147.7	−37.4	87	5.6
SU5	7/7	255/36	165.5	−47.7	56	8.1	132.5	−37.0	56	8.1
SU6	7/6	258/36	178.8	−46.7	100	6.7	142.7	−41.6	57	8.9
SU7	10/9	202/17	164.3	−48.7	34	9.0	146.1	−60.7	37	8.7
SU8	10/10	208/17	154.2	−49.2	42	7.5	136.0	−53.7	42	7.5
SU-C	9/4	262/37	170.1	−49.5	50	13.1	138.6	−33.6	50	13.1
SU-I	(9/9)		172.8	−46.4	115	4.8	138.0	−40.5	50	7.4
HTC										
SU1	9/6	269/36	194.7	−16.2	85	7.3	181.7	−22.1	83	7.4
SU2	6/6	269/36	187.4	−16.1	22	14.4	175.9	−17.7	24	14.0
SU3	8/6	268/37	182.9	−34.9	131	6.0	158.6	−29.9	131	6.0
SU-H	(8/3)		188.6	−22.4	45	18.6	172.4	−23.5	42	19.2
ITC										
BA1	8/8	105/16	177.2	−49.6	65	7.0	197.5	−51.9	62	7.2
BA2	8/8	105/15	174.5	−54.0	146	4.6	196.8	−56.7	162	4.4
BA3	8/7	91/16	169.7	−57.9	22	13.3	195.7	−57.4	24	12.5
BA4	7/7	96/21	171.6	−58.9	23	13.1	206.9	−57.6	21	13.8
BA-I	(4/4)		173.5	−55.1	303	5.3	199.1	−56.0	426	4.5
TOUR	(20/20)		174.5	−51.4	62	4.2	154.2	−36.5	11	10.4

Explanations: *B* is calculated only for the samples that were used for computation of a mean direction. TOUR, overall mean of ITC data. Other explanations as in Table 1.

[a] For single component samples only.

[b] Excluded because of low precision.

ITC found in the other sedimentary sites (KM3–7) prevails in the others (Fig. 5F). In a few samples, where both remanences co-exist, the ITC is unblocked before the "basaltic" component (Fig. 5G–H); proper isolation of the latter, however, is often prevented by the acquisition of spurious components.

As is the case for the basalt flows of sites KM8–14, the NRM of lava cobbles from the conglomerate

member (site KM-C) is dominated by a LTC. A ChRM could only be isolated from seven cobbles (Fig. 5I). These ChRM's are clearly not random, with west–northwesterly declinations and shallow negative inclinations (Fig. 6C–D).

Thus, two coherent components are isolated from this section at locality KM. One is the southward and moderately steep upward ITC in sediments that is better, but insignificantly so, clustered in situ (open squares in Fig. 6A–B; Table 2). The other remanence is a nearly horizontal and easterly component observed only in the basalt flows and in several samples of sedimentary sites KM1–2 (full and open squares in Fig. 6C–D; Table 2). A classical tilt test shows that k decreases from 17 to 10 upon untilting, which is statistically inconclusive. The in situ site-means are distributed in a girdle, so we also tried an inclination-only fold test (McFadden and Reid, 1982). This test shows a statistically significant decrease in k from 37 in situ to 11 after tilt correction. Moreover, the best grouping appears to occur in geographic coordinates for both vector and inclination-only data. Given the negative conglomerate and tilt tests, we conclude that this remanence is of postfolding origin and that two remagnetization episodes affected this section. The east–west ChRM directions of the cobbles, the basalt flows, and the sediments at sites KM1–2, are likely older than the overprint in the sedimentary sites KM3–7 as suggested by the unblocking temperatures of these two remanences at sites KM1–2 (Fig. 5G–H). The conglomerate may have been remagnetized by the

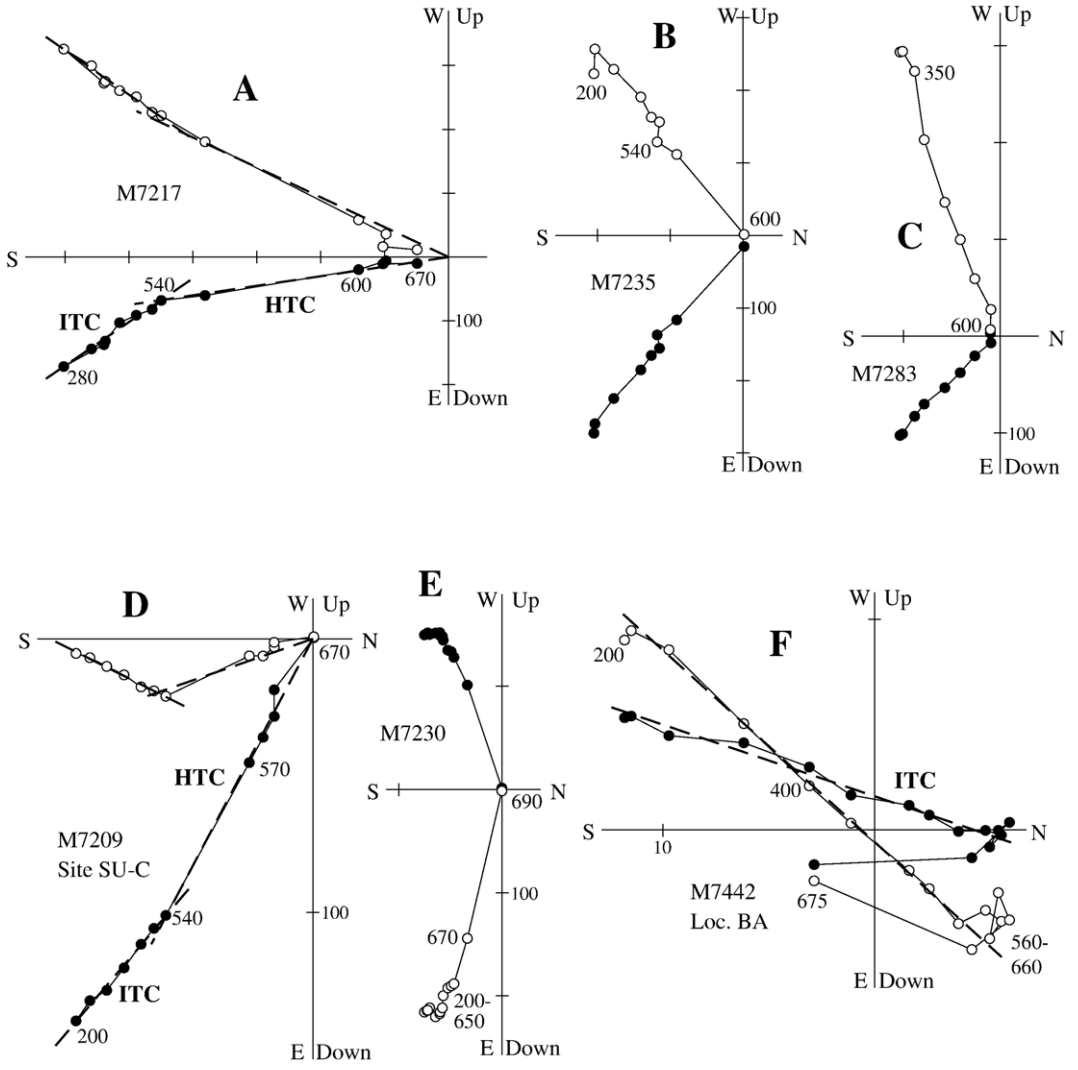

Fig. 7. Representative thermal demagnetization plots of Tournaisian rocks from localities SU (A–E) and BA (F) all in stratigraphic coordinates. (D) presents a demagnetization diagram of a sample from the conglomerate site SU-C. Other explanations as in Fig. 3.

overlying basalt pile; against this, however, speaks the exclusively normal polarity of the HTC in basalt flows opposite to the conglomerate's directions. We also recall the puzzling absence of younger overprints in the basalts. All in all, it does not look like this initially so-promising section of Fig. 5A yielded any results of possible use to us for analysis of Carboniferous tectonics. On the other hand, the ITC directions can be analyzed together with other Late Paleozoic overprints from the area.

At locality SU, two components are recognized at three sites (SU1–3) from the top of the lava section (Fig. 7A). At the structurally lower site SU4, a single isolated component slightly misses the origin (not shown), leaving a possible second component that could not be determined. At the structurally still-lower sites SU5–6, a single component is found (Fig. 7B) and the same is true for the two sites (SU7–8) of tuffaceous rocks from the second section (Fig. 7C). Two components, ITC and HTC, are present (Fig. 7D) in some lava clasts and volcanic bombs from the top of the lava section (site SU-C), while a single component is isolated from the other samples (Fig. 7E).

We use this site for a conglomerate test, although of course strictly speaking a collection of lapilli, bombs and lava blocks should not be called a conglomerate. This test is formally positive for the HTC directions, as the normalized length of the vectorial resultant sum of

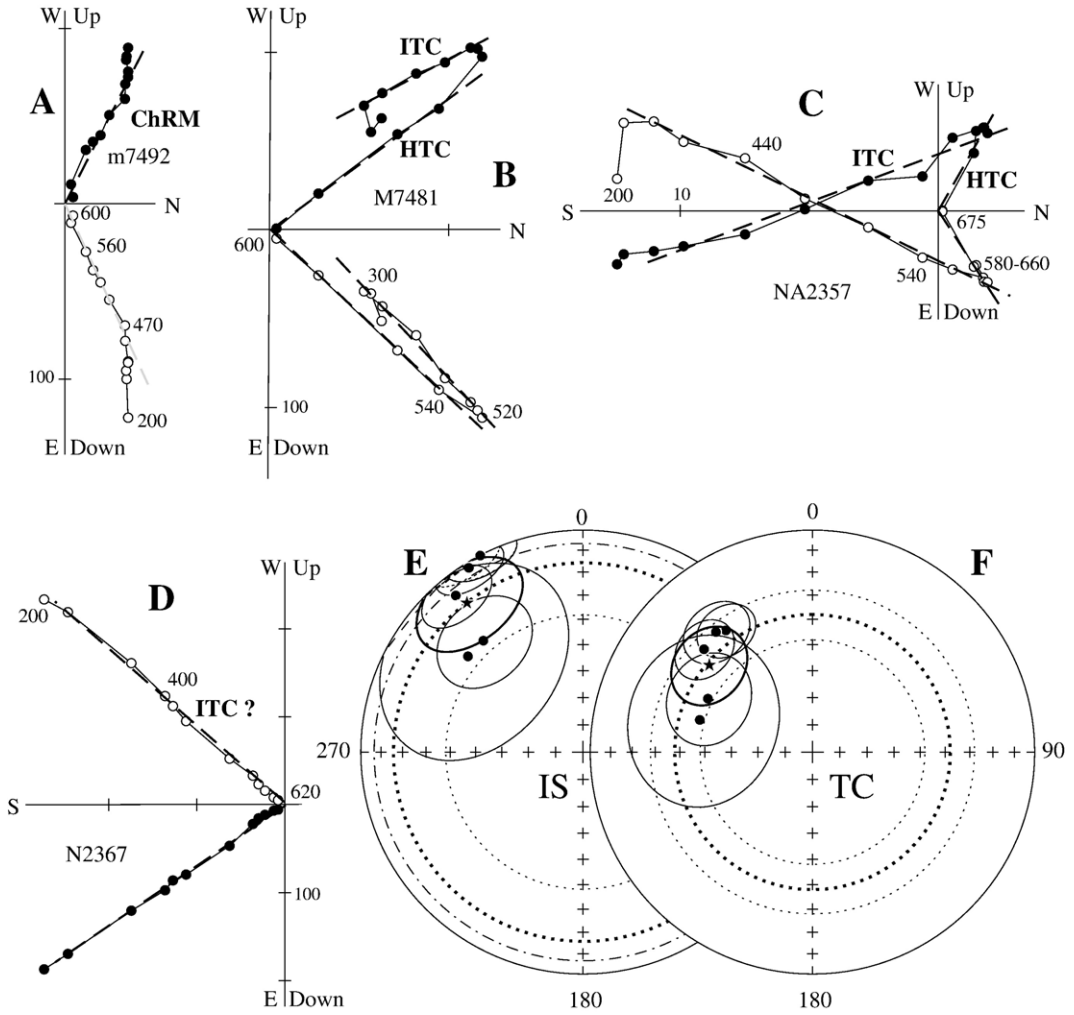

Fig. 8. (A–D) Representative thermal demagnetization plots of Bashkirian rocks from locality KC in stratigraphic coordinates. Explanations as in Fig. 3. (E–F) Stereoplots of HTC site-means (filled circles, all lower hemisphere projections) with associated confidence circles (thin lines) and the locality-mean direction (star) with associated confidence circle (thicker line). Thick dotted lines denote mean inclination obtained with the aid of inclination-only statistics with confidence interval (thin dotted and dashed-dotted line). Solid symbols and solid and dotted (dashed and dashed-dotted) lines are projected onto lower (upper) hemisphere.

0.26 is less than the 95% critical value of 0.56 of the uniformity test (Mardia, 1972). Visual inspection of the data, however, shows that the distribution is not perfectly random, and that all eight SU-C HTC vectors lie in the lower hemisphere (Fig. 6E).

The ITC directions from the section top, the overprints in the conglomerate, as well as those of the ChRM's at other host-rock sites, are clearly secondary, as evidenced by a negative fold test (see open circles in Fig. 6A–B) and clustering of directions in the clasts (Table 2). The fold test is inconclusive for the HTC isolated from sites SU1–3 (Table 2). Thus we have just three Tournaisian sites from locality SU where the HTC may be primary, but the lack of the fold test, a dubious conglomerate test, and the limited statistical significance renders this result unreliable.

At locality BA, the NRM of several of the redbed samples is dominated (not shown) by a single ChRM component that decays to the origin, but in other samples this same directional component is an ITC and bypasses the origin (Fig. 7F). An HTC is clearly present but could not be reliably determined because of the acquisition of spurious magnetizations. Limited variation in bedding attitudes renders the fold test inconclusive for the ITC component (see Table 2), but it is clear that this ITC is a secondary magnetization.

At locality KC, the NRM is dominated by a downward-directed ChRM of normal polarity at some sites (Fig. 8A), while a reversed ITC and normal HTC could be isolated at others (Fig. 8B–C). At site KC 6, a single well-defined ChRM component is present, but in contrast to other sites, this direction is of reversed polarity (Fig. 8D), so we take it to be of the same "vintage" as the ITC shown in Fig. 8B and C. When we include this site-KC 6 result with the ITC directions, the fold test for the three sites suggests a prefolding origin of this remagnetization (Table 3).

The best grouping of the HTC directions is achieved after complete tilt correction (Fig. 8E–F), but the improvement is statistically insignificant. These five tilt-corrected site-means show a spread in declinations but display similar inclinations (Fig. 8F). We therefore performed an inclination-only tilt test (McFadden and Reid, 1982), which is positive (Table 3), with maximum data grouping in stratigraphic coordinates. Thus this component also predates tilting.

4.3. Data summary

Reversed ITC directions from Upper Permian localities KB and KP in the Junggar–Alatau Range show significant improvement in data grouping upon tilt correction (Fig. 4A–B; Result TR in Tables 1 and 4). Minimum dispersal ($kappa_{max}$) is reached at 100% unfolding, thus testifying to a prefolding age for this secondary remanence.

The combined Late Permian ChRM+HTC results from localities BO, KP, and KB converge upon tilt correction in a positive tilt test for $N=19$ sites. The five SH site-mean directions deviate, mostly in declination, but also partly in inclination (Fig. 4C–D; Table 1). Analyzing the results from all Upper Permian sites ($N=24$) from these four localities, an inclination-only fold test (McFadden and Reid, 1982) appears to be positive — see result PER at the bottom of Table 1. A disturbing feature, however, is that the maximum in data

Table 3
Mean directions in Bashkirian (Lower Pennsylvanian) rocks from the Junggar–Alatau Range

S/L	*N*	B	In situ				Tilt-corrected			
			D°	I°	*k*	$\alpha_{95°}$	D°	I°	*k*	$\alpha_{95°}$
ITC										
KC1	7/6	186/41	168.4	1.9	66	8.3	163.8	−36.9	66	8.3
KC5	9/5	176/29	165.4	−4.0	43	11.8	163.5	−32.5	42	12.0
KC6	8/5	137/23	160.5	−23.8	36	12.9	167.7	−44.3	36	12.9
KC-I	(6/3)		164.9	−8.6	34	21.6	164.9	−37.9	169	9.5
HTC and ChRM										
KC1	7/7	186/41	332.4	0.1	41	10.2	324.6	33.2	41	10.2
KC2	8/4	183/36	328.3	2.7	84	10.1	321.2	31.2	64	11.6
KC3	8/4	191/28	318.2	33.2	30	16.9	297.1	46.1	33	16.2
KC4	4/3	184/30	309.8	33.1	35	13.7	286.0	46.2	48	11.7
KC5	9/5	176/29	321.0	10.1	53	11.4	313.5	33.2	59	10.7
KC-H	(6/5)		322.5	15.9	20	17.6	309.9	38.9	31	14.0
INCL	(6/5)		–	15.8	12	25.9	–	38.0	58	11.8

INCL is obtained with the aid of inclination-only statistics (McFadden and Reid, 1982). Other explanations as in Table 1.

Table 4
Summary of Permian paleomagnetic results from the Devonian and Late Paleozoic strongly curved volcanic belts

Data	C	SC	D°	I°	α_{95}°	$R \pm \Delta R$	References
NE arm							
1a	P	s	265	−50	5	−25±8	Levashova et al. (2003a)
1b	P	s	237	−48	3	3±6	Levashova et al. (2003a)
2	O	g	246	−57	10	−6±16	Collins et al. (2003)
3	O	g	246	−72	11	−7±31	Levashova et al. (2003b)
4	O	g	248	−71	4	−8±12	Levashova et al. (2003b)
SW arm							
TR	O	s	171	−65	7	63±18	This paper
BO	P	s	152	−40	5	84±7	This paper
SH	P	s	208	−40	13	28±15	This paper
KP-H	P	s	157	−51	7	79±10	This paper
KB-H	P	s	322	51	6	94±8	This paper
KM-I	O	g	178	−56	10	58±15	This paper
SU-I	O	g	167	−46	5	69±7	This paper
BA	O	g	174	−55	5	62±9	This paper

Entries are numbered as in Fig. 10. Entries 1a and 1b represent prefolding directions from two Upper Permian localities; 2, 3, and 4, postfolding overprints in Ordovician, Silurian and Devonian rocks, respectively. C, paleomagnetic component, in which P is prefolding and presumably primary, whereas O denotes an overprint of likely Late Paleozoic age.
SC, coordinate system in which the result is presented: g, geographic; s, stratigraphic.
$R \pm \Delta R$, rotation angle (positive if counterclockwise) with its confidence limits calculated as suggested by Demarest (1983); all rotations are computed with respect to the 270 Ma pole for Europe (Torsvik et al., 2001), except for the entry TR, where the 240 Ma pole is used. Other explanations as in Table 1.

grouping ($kappa_{max}$) occurs at 85 to 90% unfolding. This could indicate an unresolved postfolding contamination, but the perfectly rectilinear decay observed over wide temperature intervals in the demagnetization diagrams for most samples (Fig. 3) renders this assumption unlikely. A more likely, but also not unique, explanation is to attribute this feature to unrecognized primary tilts, which are plausible in these subaerial volcanic rocks. The rocks from these four Upper Permian localities are broadly coeval, given the palynological data and the more alkalic composition of the volcanics compared to those of the older rocks, which is generally taken as characteristic of a Late Permian age (Koshkin, 1974; Bekzhanov et al., 2000). The normal polarity of the HTC at locality KB indicates that the Late Permian volcanism continued beyond the Upper Kiaman boundary, indicating that these results represent the geomagnetic field of ~260 My; they are included in Table 4 as four separate, presumably primary magnetizations (labeled BO, SH, KP-H and KB-H, where H=HTC).

The tilt test indicates a post-tilting origin for the reversed ITC directions in the Tournaisian rocks of locality SU and is inconclusive for the results from the other two Tournaisian localities separately (KM and BA in Table 2). Combined overprint data from localities KM, SU and BA (N=20 sites) show a ca. six-fold drop in dispersion upon tilt correction; in Table 2 this combination is labeled TOUR. These ITC entries for the three localities are labeled KM-I, SU-I and BA in Table 4 and are listed without tilt corrections (i.e., in geographic coordinates). During incremental unfolding, a maximum clustering at 10% unfolding exceeds the in situ value by less than 10%.

The HTC directions from locality KM (Table 2) do not pass a fold test either. We infer that these Tournaisian rocks were remagnetized, but cannot determine at what stage in the deformation, nor do we know at what time; consequently, these results are nearly useless and will not be used in the tectonic analysis. The HTC directions from locality KC (Table 3) are of normal polarity (Fig. 8E–F) and could be primary, but the fold test is not significant. We do include the HTC results for localities SU and KC in our analysis below, but realize that they can only form a preliminary basis for tectonic conclusions.

5. Comparison of the observed directions with those extrapolated from Baltica

As described in Section 1: Introduction, the volcanic belts of Kazakhstan have strongly curved outlines in planar view, which may be a result of oroclinal rotations. To test whether rotations occurred, paleomagnetic declinations should be compared with reference declination values; in our case, we opt to extrapolate from the paleopoles from Baltica, because the paleolatitudes derived from Kazakhstan's magnetizations and those extrapolated from Baltica agree to first-order (Bazhenov et al., 2003; Collins et al., 2003; Levashova et al., 2005). Following these comparisons with Baltica, we will also compare declination values from different areas *within* the Kazakhstan curved belts with each other, in order to examine oroclinal bending.

The precise ages of many magnetizations, in particular the secondary overprints, are poorly known or have been inferred from inclination comparisons and tilt or fold tests. Thus, some error may be introduced into the computation of declination deviations (i.e., relative rotations). We note, however, that the expected inclinations, extrapolated from Baltica to the study area, steadily increase with age during the Late Paleozoic, whereas the declinations show relatively minor changes (Fig. 9). Hence, the age-related errors are small

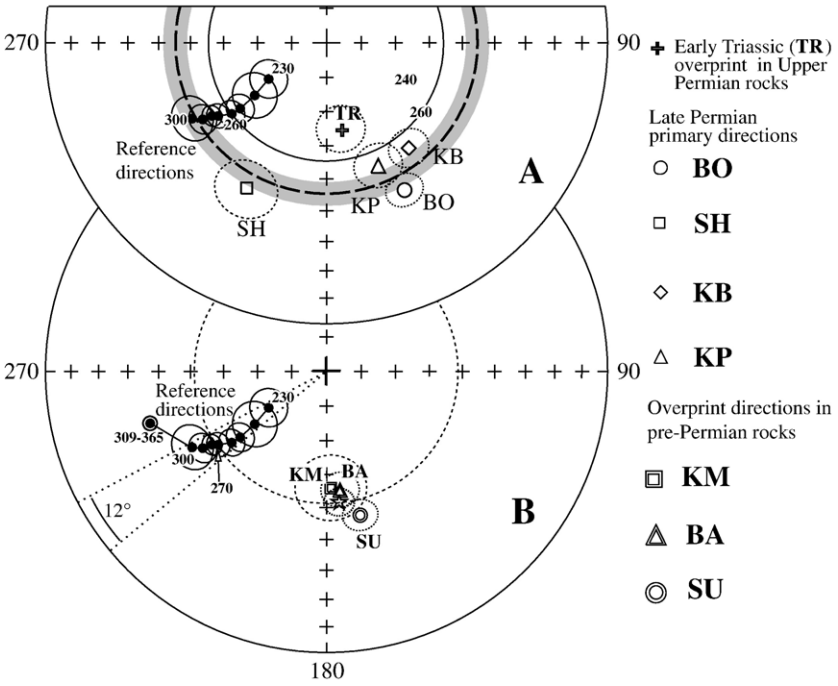

Fig. 9. Stereoplots of the reference and observed locality-mean directions. Reference data (as solid circles, which are in the upper hemisphere and are shown with ages in Ma) with associated confidence circles (thin solid lines) are calculated by extrapolation from the APWP of Baltica (Torsvik et al., 2001) for a common point in Kazakhstan at 43° N, 80° E; only reference directions for 10 Ma intervals are shown for clarity. Encircled solid dot (in B only) is the Early Carboniferous reference direction recalculated from the APWP of Baltica of Van der Voo (1993). (A) Mean prefolding Early Triassic overprint direction and Late Permian locality-mean directions with associated confidence circles (dashed lines). The data are labeled as in the text and Table 1. The mean direction for locality KB has been inverted. Thick dashed line, overall observed Late Permian inclination calculated with the aid of inclination-only statistics with its confidence interval (shaded). For easy reference, a thin solid line that is centered on the projection pole shows the inclination value for 260 Ma. All observed directions are in stratigraphic coordinates. (B) Locality-mean overprint directions in Tournaisian rocks with associated confidence circles (dashed lines). The data are labeled as in the text and Table 2. Thin dashed line, circular about the figure's pole, represents the overall mean inclination from the Tournaisian data so that it can be compared with the reference directions. Dotted lines, emanating from the projection center, denote the variance in reference declinations (12°) for the interval 230–300 Ma. All observed directions are in geographic coordinates. All symbols and lines are projected onto upper hemisphere.

compared to the magnitude of the first-order pattern of rotations that we wish to establish. We use the declination calculated by extrapolation from the 270 Ma pole for Europe (Torsvik et al., 2001) as the reference for all Permian data and the overprints, except for the entry TR where the 240 Ma pole is used in order to compute $R \pm \Delta R$ in Table 4 (Demarest, 1983). We used the 309–365 Ma mean paleopole for Baltica from Van der Voo (1993) as representative of the Mississippian–earliest Pennsylvanian (Bashkirian) in the new time scale (Gradstein and Ogg, 2004). Thirdly, we used the 440 Ma mean paleopole for Baltica from Cocks and Torsvik (2002) as a reference pole to compare with previously published results from the Late Ordovician (Bazhenov et al., 2003; Collins et al., 2003; Alexyutin et al., 2005a).

Examining the range of reference directions in Fig. 9, it can be seen that the 240 Ma reference inclination best matches that of the prefolding reversed overprint in localities KB and KP (labeled TR); thus, we assign an Early Triassic age to this remanence. The postfolding reversed overprint inclinations in the Tournaisian rocks (KM, BA and SU in Fig. 9B) match the reference inclinations with an age of 270–280 Ma, indicating a mid-Permian age for this remanence.

The Late Permian overall inclination (averaged from the presumably primary directions from the four localities BO, KB, KP and SH) is shallower by 8.4°±3.6° than the 260 Ma reference value and best agrees with the 290 Ma (Early Permian) reference inclination (Fig. 9A). Such an age, however, contradicts stratigraphic data (Skrinnik and Grishina, 1997) and the observed normal polarity at locality KB. We assume that minor (and therefore unrecognized) primary tilts are possible explanations for this shallowing of the inclination in these subaerial volcanics.

Pretilting, presumably primary Permian results from the northern limb of the Late Paleozoic volcanic belt (results 1a and 1b, Table 4, and Fig. 10) come from two localities about 50 km apart (Levashova et al., 2003a); one locality-mean declination shows a clockwise rotation of 25°±8°, while the other locality has a declination that agrees with the Baltic reference direction within error-limits. Levashova et al. (2003a) attributed the apparent rotation of the first locality to local tectonics and concluded that no large-scale rotation occurred in the Chingiz Range of NE Kazakhstan since the Late Permian. Post-tilting overprints in Lower to Middle Paleozoic rocks in this region (Collins et al., 2003; Levashova et al., 2003b) are likely to have been acquired during the reversed Kiaman superchron judging by their steeply upward inclinations and exclusively reversed polarity. These secondary magnetizations (Localities 2–4, Fig. 10, Table 4) also show little or no rotation with respect to the reference direction and corroborate the above conclusion.

Further to the northwest, Late Paleozoic overprints of reversed polarity were reported from Devonian volcanics (Grishin et al., 1997). However, these authors obtained dispersed distributions of high-temperature components in these rocks and selected only those close to the expected Late Paleozoic directions as overprints. By definition, the mean directions so obtained cannot reveal any rotation and cannot be used in this study.

All primary and overprint directions from our present study area in the SW arm of the belts are rotated counterclockwise (ccw) with respect to Baltica's reference declinations. For the results from this study, except SH, these rotations range from about 60° to more than 90° (Table 4). The SH locality displays a ccw rotation of 28±15° (Table 4; Figs. 9 and 10).

This pattern suggests a nearly homogeneous rotation for the entire sampling area, with the SH result a local anomaly. However, other areas in the North Tien Shan, to the east or west of our study area, and even the Tarim block to the south seem to display counterclockwise

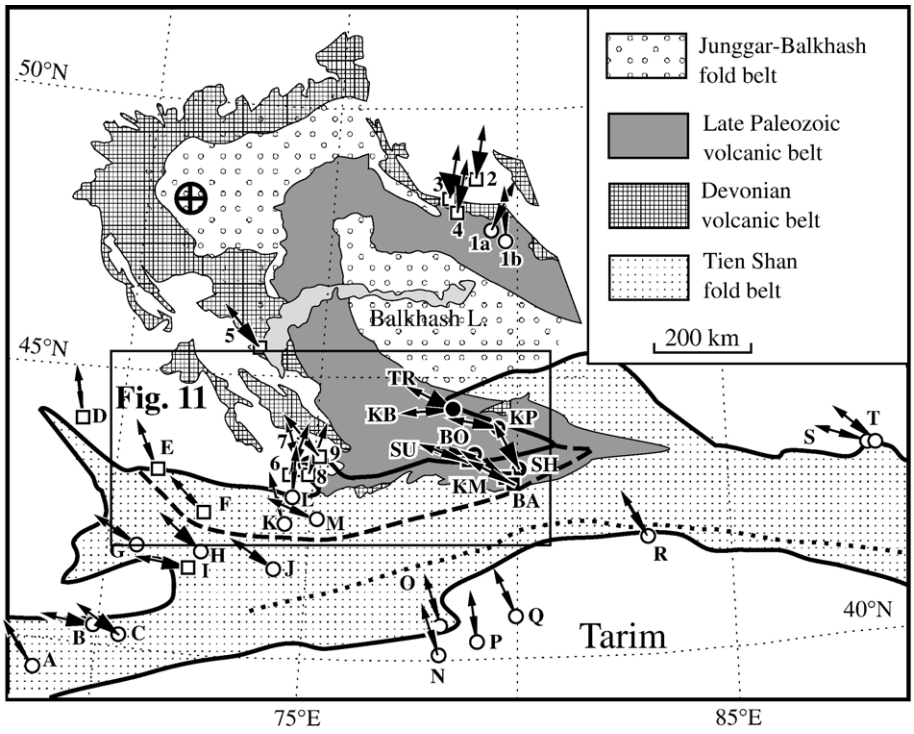

Fig. 10. Geological map showing the relationship between the strongly curved Devonian and Late Paleozoic volcanic belts of Kazakhstan (shaded) and the Tien Shan fold belt, as well as the localities where Permian and Triassic magnetizations have been documented. Arrows represent declination deviations (interpreted as rotations about vertical axes) from the reference declination calculated from Baltica's APWP for the area; given that the arrows are plotted with respect to the present-day meridians, a north-pointing arrow denotes zero deviation and no rotation. Black sectors denote confidence limits of the rotation angle. The boundaries of the Tien Shan fold belt are shown by the thick solid lines; separately delineated is the North Tien Shan zone (thick dashed line). The thick dotted line is the oceanic suture in the central and eastern parts of the Tien Shan (simplified after Biske (1995)). The localities where primary (secondary) components are found are shown by circles (squares); solid and open symbols denote the results of this study and published data, respectively. Data are labeled as in Tables 4 and 5. The large crossed circle in the northwestern part of the map denotes a hypothetical Euler rotation pole (see text for discussion).

Table 5
Published Permian and Triassic results from the Tien Shan and adjacent areas

Data	C	D°	I°	$R° \pm \Delta R°$	Reference
5 (SAR)	O-g	188	−66	46±13	Alexyutin et al. (2005b)
6 (AGA)	O-g	250	−57	−16±9	Alexyutin et al. (2005b)
7 (GEO)	O-g	215	−51	19±10	Alexyutin et al. (2005b)
8 (ODA, OTA)	O-s	250	−44	−16±11	Alexyutin et al. (2005b)
9 (ESP)	O-g	189	−37	45±10	Alexyutin et al. (2005b)
A	P	188	−48	41±6	Bazhenov et al. (1993)
B	O	322	43	87±14	Bazhenov et al. (1999)
C	P	355	70	60±16	Bazhenov et al. (1993)
D	O	216	−42	16±4	Bazhenov et al. (1995)
E	O	205	−50	28±64	Bazhenov et al. (2003)
F	O	185	−51	8±8	Bazhenov et al. (2003)
G	P	350	56	60±8	Bazhenov et al. (1999)
H	P	178	−58	53±11	Bazhenov et al. (1999)
I	O	330	51	82±12	Bazhenov et al. (1999)
J	P	173	−44	61±10	Bazhenov et al. (1999)
K	P	213	−49	22±5	Audibert and Bazhenov (1992)
L	P	235	−46	1±4	Audibert and Bazhenov (1992)
M	P	163	−48	73±8	Audibert and Bazhenov (1992)
N	P	208	−50	24±7	Li et al. (1988)
O	P	212	−58	24±5	Sharps et al. (1989)
P	P	222	−50	14±5	Bai et al. (1987)
Q	P	214	−41	22±6	Bai et al. (1987)
R	P	202	−55	33±9	McFadden et al. (1988)
S	P	163	−62	74±8	Sharps et al. (1992)
T	P	187	−59	51±10	Nie et al. (1993)

Entries are numbered as in Fig. 10 and labeled approximately from west to the east.
Entries 5–9 are overprints of reversed polarity from Alexyutin et al. (2005a,b); locality-identifying labels are added in parentheses; their results are presented in g = geographic coordinates, or s = stratigraphic coordinates. Other explanations as in Table 4.

rotations as well, so we will next examine previously published Late Paleozoic paleomagnetic data from areas mostly outside the curved Late Paleozoic volcanic belt (see Fig. 10); these results are listed in Table 5. For this analysis only results based on complete demagnetization and principal component analysis were considered. We excluded all sites in these previous studies that had a 95% confidence circle with radius >20° as well as localities based on only three site-means or less; where necessary, we recalculated locality-mean directions.

Ordovician to Carboniferous redbeds and volcanics were studied by Alexyutin et al. (2005a,b; pers. comm. 2005) within and close to the SW limb of the strongly curved Devonian volcanic belt (see Fig. 10). These studies revealed reversed post-tilting overprints in four Lower and Middle Paleozoic formations and one pretilting overprint in Carboniferous rocks. Because these magnetizations (#5–9 in Table 5 and Fig. 10) are reversed, we consider them as acquired during the Kiaman reversed superchron and hence broadly coeval with our results. Dual-polarity and normal polarity post-tilting overprints are found at several other localities (Alexyutin et al., 2005b; pers. comm. 2005); the ages of these magnetizations, however, are uncertain and debated, so we exclude them from the analysis. Among the five results from this region west of our study area, the overprint declination from locality 5 near Balkhash Lake shows a large ccw rotation similar to most other results from SE Kazakhstan, whereas the other four reversed overprints show rotations, either ccw or cw, without any prevailing trend (#6–9, Table 5, Fig. 10).

Many other Permian and Triassic results are available from the Tien Shan and adjacent areas (Fig. 10; entries labeled A–T in Table 5). With only one exception, all these results show significant ccw rotations, which range from small (~15°) in northern Tarim and SW Kazakhstan to large (close to 90°) in other areas (Table 5; Fig. 10). The only exception in the Tien Shan that reveals a statistically zero rotation is result *L* (Table 5, Fig. 10) from approximately the same area where the data of Alexyutin et al. (2005a,b) come from; this area (called the Kendyktas block) thus shows an unsystematic rotation pattern as already mentioned.

Apparently, the Late Paleozoic data from the North Tien Shan and adjacent areas such as the Ili River Valley in the present study, represent considerable and more or less systematic counterclockwise rotations after the Late Permian. With respect to Baltica, these rotations are large and counterclockwise (up to ~90°). In contrast, in the northern limb in the Chingiz area north of Lake Balkhash, the rotations are generally small and predominantly clockwise (Fig. 10).

The Mississippian and Early Pennsylvanian results from our study area in the North Tien Shan are from localities KC–KP (combined), and SU (HTC directions); they are rotated ccw by 85° and 128° with respect to the Baltica reference declination.

The latest Ordovician (~440 Ma) paleopole from Baltica (at 5° N, 187° E; Cocks and Torsvik, 2002) predicts a declination of 70° for the Kazakhstan areas, if they had rigidly belonged to Baltica since that time. It is not surprising of course that this "rigid belonging" is falsified by the observed southerly declinations in the Chingiz Range (Collins et al., 2003) and the generally northerly declinations in the North Tien Shan (Bazhenov et al., 2003; Alexyutin et al., 2005a). We can conclude from this that a post-Ordovician cw rotation of about 100° occurred for Chingiz, and a ccw rotation of about 70° for the North Tien Shan, with respect to Baltica's reference value. Note that because of the observed spread in declinations in the rocks from the North Tien Shan, where Late Ordovician declinations vary between 337° and 31°, the magnitude of the overall rotation with respect to Baltica's reference values cannot be estimated very precisely.

In summary of this section, we realize that minor discrepancies exist between the observed and reference inclinations extrapolated for the Permian from Baltica, but argue that these do not invalidate the latitudinal agreement to first approximation. Moreover, a similar agreement exists for Permian and Triassic inclinations from other parts of the Tien Shan and adjacent areas, the Tarim block in particular (Bazhenov et al., 1993; Gilder et al., 1996; Bazhenov et al., 1999). In contrast, the declinations show deviations for the Permian that are so large that they cannot be attributed to minor primary bedding dips or age uncertainties on the order of a few tens of millions of years. Hence, the Baltic reference values can be used for an evaluation of post-Permian rotations in Kazakhstan. Comparisons of Early Carboniferous and Ordovician results with Baltica reference declinations show large counterclockwise rotations for the North Tien Shan, in similar fashion as the Permian results of Fig. 10.

6. Rotations as a function of time and relative rotations between different areas

The previous section illustrates, clearly, that a uniform post-Permian rotation of the entire Late Paleozoic curved volcanic belt in Kazakhstan is not supported. Large counterclockwise rotations are observed in Permian rocks in many areas along the North Tien Shan range, whereas no (or only minor, often clockwise) rotations are observed in the already mentioned Kendyktas block and in the Chingiz area.

Mississippian and Early Pennsylvanian (Bashkirian) rocks accumulated during the early stages of the Late Paleozoic belt evolution in the North Tien Shan. One might expect that results for this time interval would reveal paleomagnetic declinations that are equally or even more ccw rotated than the Permian ones. There are five areas in or near the southern limb of the Late Paleozoic belt where pairs of Carboniferous–Permian data are available (Fig. 11 and Table 6). The results from the present study (localities KP–KC and SU) have been compared already with the reference declination

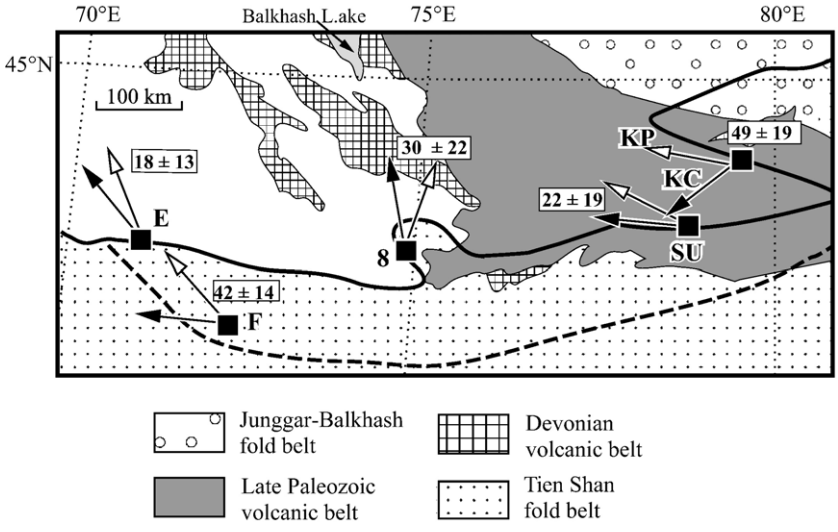

Fig. 11. Distribution of localities where pairs of Carboniferous and Permian data are available. Localities are labeled as in Fig. 10 and Tables 4, 5 and 6. Arrows with solid (open) arrowheads denote Carboniferous (Permian) observed directions. Framed numbers show the angular differences in declination (all are positive, meaning that the older direction is counterclockwise rotated with respect to the younger one). Confidence limits have been computed as suggested by Demarest (1983). Other explanations as in Fig. 10.

Table 6
Comparison of rotations deduced from Carboniferous and Permian data

Data	D_m°	R_P°	R_C°	R_C–R_P°	Reference
SU-I	353	63±7		22±19	This paper
SU-H	352		85±23		
KP-H	337	79±10		49±19	This paper
KC-H	310		128±21		
F(ITC)	5	48±8		42±14	Bazhenov et al. (2003)
F(HTC)	344		90±16		
E(ITC)	25	28±6		18±13	Bazhenov et al. (2003)
E(HTC)	28		45±16		
8(ITC)	70	−16±11		30±22	Alexyutin et al. (2005b)
8(HTC)	61		14±25		

Localities (components) are labeled as in Tables 2, 4 and 5 and Figs. 10 and 11; D_m, measured mean declinations; R_P, rotation with respect to the 270 Ma Baltica reference direction; R_C, rotation with respect to the 337 Ma Baltica reference direction; R_C–R_P, rotation during the Early Carboniferous–Late Permian interval.

extrapolated from Baltica in the previous section; other previously published and presumably primary results from Early Carboniferous rocks and their ubiquitous Permian overprints (labeled 8, E and F in Figs. 10 and 11 and Table 6) are included also.

In the previous section, we discussed the corresponding rotations with respect to the 270 Ma and 337 Ma Baltic reference declinations, and now we turn to comparisons between the different areas in eastern Kazakhstan. These comparisons, importantly, also allow us to test whether rotations of a given area occurred as a function of time, in addition to rotations between areas. One can see in Table 6 that in all five cases from the North Tien Shan there were significant rotations (column R_c–R_p) during the Early Carboniferous–Permian interval and that these rotations are of the same sense as the post-mid-Permian rotations (Table 6). Fig. 11 illustrates the rotations indicated by Upper Permian results (open-tipped arrows) and those observed in Early Carboniferous rocks (filled arrows), and it is seen that in all cases the latter are more rotated than the former and that the differences are systematic, in accord to what is expected for protracted rotation processes during the Late Paleozoic.

Unfortunately none of the previously published results from Devonian rocks are of undisputable quality, so that our only other kinematic indicators come from Ordovician–Silurian paleomagnetic data from the North Tien Shan and the Chingiz range (Bazhenov et al., 2003; Collins et al., 2003; Levashova et al., 2003b; Alexyutin et al., 2005a). Levashova and co workers (2003b) concluded that the northern limb of the volcanic belts was rotated (probably after the Middle Devonian), by approximately 180° with respect to a more or less unrotated southern limb. Thus, while the post-Permian relative rotations between the Chingiz Range and North Tien Shan are on the order of 90°, the post-Ordovician relative rotations between these two areas amount to about 180°. This implies that about half of the post-Ordovician rotations had occurred before the Late Permian.

We conclude this section by summarizing that the kinematics we deduce from the declination patterns in the Paleozoic rocks of the curved Devonian and Late Paleozoic volcanic belts of Kazakhstan thus include (at least) two phases of rotation: (1) after the Ordovician, and before the Late Permian a total of some 90° of *relative* rotation occurred between the northern (Chingiz) and southern (North Tien Shan) limbs, followed by (2) a phase of rotations occurring during the Late Permian–Early Mesozoic interval during which another 90° of *relative* rotation occurred. Fig. 11 illustrates that with good data coverage, some of the ages and amounts of rotations may be further constrained, but our coverage is still far from complete enough to speculate further.

7. Discussion of the Late Paleozoic dynamics in the region

In any paleomagnetic study, it is always simpler to reach a kinematic inference than to arrive at an understanding of the plate tectonic forces (the dynamics) that produced the kinematic patterns. Central Asia in Late Paleozoic–Early Mesozoic time is a particularly difficult space–time situation, because our knowledge of the relevant tectonic scenarios is still largely incomplete.

To explain the rotations of one or the other limb, either relative to Baltica, or relative between the two limbs, we could envision the following dynamical causes:

1. Oroclinal bending, a process in which an originally straight belt becomes curved. Typically variations in strike along the belt match variations in declination in an orocline. Thus, a test of oroclinal bending consists

of gathering sufficient declination data along the belt. Moreover, in terms of the dating of the oroclinal bending, it is necessary to have sufficient well-dated results of the right ages to determine when the process took place. If the curvature of a belt is large, solutions must present themselves to eliminate material in between the limbs to accommodate the increasing space problem in the interior of the tightening arc.

2. Block rotations, a process in which a number of relatively rigid blocks slide past one another along curved faults, so as to produce significantly deviating declinations. The process can involve large or small blocks, although it is much easier to envision the effect of small block rotations in the case of a mobile belt like the Altaids, because large blocks with dimensions of some 1000 km or more obviously need "room to maneuver".
3. Wrench-faulting, a mechanism in which a dominant set of strike-slip faults, possibly accompanied by a conjugate set of strike-slip faults with offsets in the opposite sense, produce drag — i.e., rotations along vertical axes in the vicinity of the fault traces, that correspond to the sinistral (ccw) or dextral (cw) sense of relative movement. This mechanism may include plate boundary processes in the case of strongly oblique continent–continent collisions.

A discussion of the three possibilities listed above (or any combination thereof) needs to take into account that the domains of Kazakhstan, the Tien Shan and Tarim have long been known to have become "continentalized", by which we mean that marine conditions had disappeared from the entire region, by Early Permian time or even earlier. So, generally, scientists have maintained that these elements were already welded together before the Guadelupian, i.e., about 270 Ma or even earlier (e.g., Zonenshain et al., 1990; Chuvashov, 1999), and that by then the consolidated continental crust of northern Eurasia had formed. Oceanic basins between the Tarim block, on the one hand, and the North Tien Shan and Kazakhstan, on the other, were thus mostly closed before the Late Pennsylvanian, with their last traces disappearing by the beginning of the Permian (Biske, 1995). Such major deformation as connected by most authors with the closure of an oceanic basin thus took place in the Junggar–Balkhash fold belt by the Carboniferous–Permian boundary (Bekzhanov et al., 2000). Note also that both strongly curved Devonian and Late Paleozoic belts of Kazakhstan unconformably overlap older tectonic structures, but that no tectonic sutures and/or major zones of deformation are recognized between the belts and adjacent areas.

If the rotations involved a single large-block, such as delineated by all the ccw rotations in Fig. 10, the length of this block would be about 1500 km and a significant rotation, say 45°, of the North Tien Shan and Tarim Craton combined would, of necessity, produce convergence (and elimination of an intervening ocean?) of some 1000 km or more. This is much too large to be sustained by geological data. Thus, we need to break up this long block in smaller units, behaving as ball-bearings in a shear zone. But no evidence is available for this scenario either. For instance, the oceanic suture between Tarim and the orogenic belt that is now traced over more than 1000 km in the central and eastern parts of the Tien Shan (Fig. 10) would have been torn apiece. We are, therefore, forced to consider really small blocks or localized rotations and will do so, when we discuss wrench-fault systems.

Oroclinal bending, similarly, poses large problems. If the Tien Shan were involved in oroclinal bending of the strongly curved Devonian and Late Paleozoic volcanic belts, post-mid-Permian motions of this entire looping belt (about 2500 km long) would be required. The corresponding rotation (Euler) pole should be somewhere in central Kazakhstan in order not to disrupt the pre-rotational structural features and links, including the volcanic belts themselves (Fig. 10). Moreover, Baltica reference and observed paleolatitudes show good agreement for the present-day orientation of the Tien Shan (Bazhenov et al., 1999; Levashova et al., 2005). The ccw rotation of the southern arm during oroclinal bending requires compression in the inner parts of the curved volcanic belts, i.e. in the Junggar–Balkhash fold belt, and the inherent age of the related deformation must fit that indicated by paleomagnetic data. But as noted before, major folding and thrusting in this domain took place by the Carboniferous–Permian boundary (Bekzhanov et al., 2000), whereas the rotated Late Permian and Triassic directions in the Tien Shan (McFadden et al., 1988; Bazhenov et al., 1993; this study) indicate a much younger rotation age. Permian rocks are indeed deformed in the Tien Shan and Kazakhstan, but the late orogenic gentle folds and rare low-magnitude thrusts can account only for minor shortening. Thus there is no deformation to accommodate the convergence between the two limbs of the curved Late Paleozoic belt of Fig. 1 that would be expected for large-scale post-Paleozoic oroclinal bending.

Hence we conclude that the bulk of the observed ccw Late Permian–Early Triassic rotations in the SW limb of the Late Paleozoic volcanic belt cannot be related to large-scale (~90°) oroclinal bending and should be

accounted for in a different way. Oroclinal bending may, of course, have contributed to the pre-Pennsylvanian rotations in South Kazakhstan or the North Tien Shan (as well argued by Şengör and Natal'in, 1996) but it fails to give an explanation for the large (~90°) rotations of Late Permian–Triassic age in central Asia (Fig. 10).

More appealing appears to be the idea that distributed deformation affected the region. Bazhenov et al. (1999) hypothesized that a sinistral wrench zone paralleled the western part of the Tien Shan in the latest Permian–Triassic; geological data supporting this view are now available from the Kyrgyz part of the Tien Shan (Bazhenov and Mikolaichuk, 2004). In adjacent Chinese parts of the Tien Shan, Permian strike-slip movements along the Main Tien Shan Fault are dextral (Laurent-Charvet et al., 2003), but Wartes et al. 2002 (p. 148) stated that these dextral movements had stopped after the Early Permian, followed by a reversal of strike-slip kinematics. This matters for our interpretation of the paleomagnetically determined rotations as of Late Permian–Early Mesozoic age. Natal'in and Şengör (2005) adopted a large-scale sinistral wrench-faulting, as illustrated in Fig. 12, where Siberia and Baltica are seen to converge in a large-scale sinistral system that shears Kazakhstan and rotates Tarim ccw, as is indeed observed both in terms of paleomagnetic declinations and local geology (Allen et al., 1995; see also Şengör and Natal'in, 1996). This contrasts with an earlier conclusion that the main cratonic blocks (Baltica, Siberia, Tarim) and the Ural–Mongol belt had already

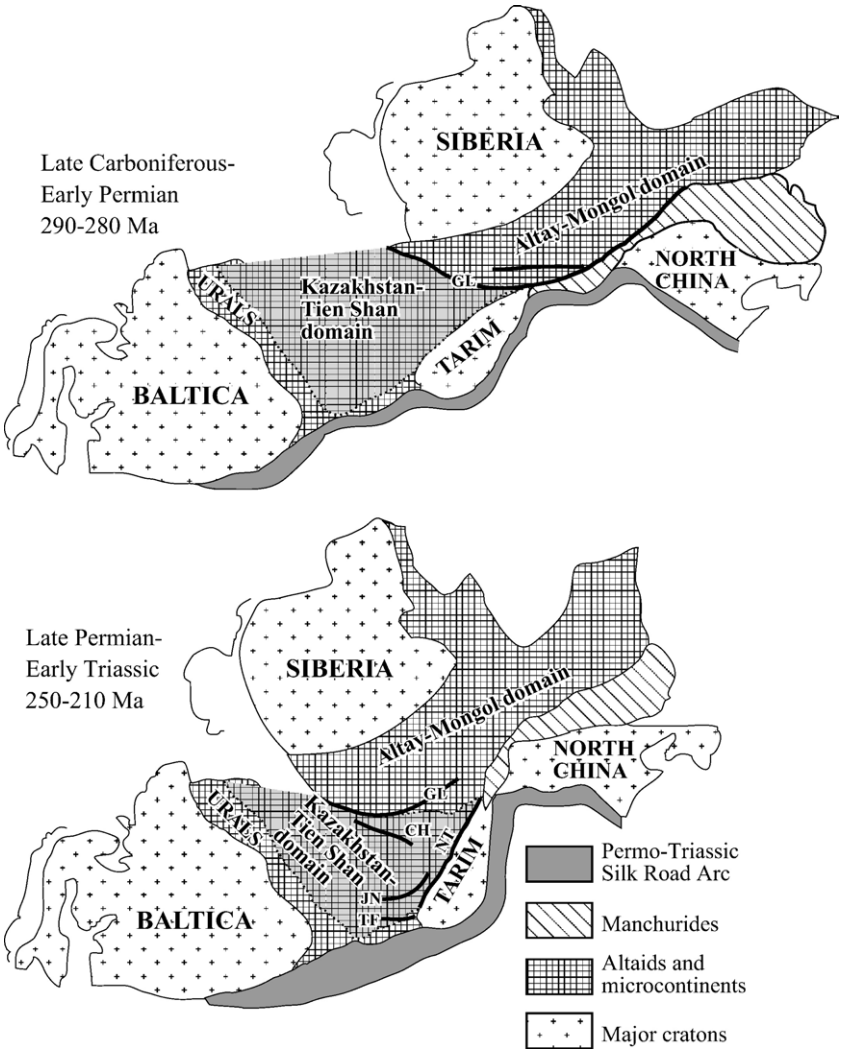

Fig. 12. Late Paleozoic sinistral transpression between the converging Siberia and Baltica cratons, hypothesized as causing predominantly counterclockwise rotations in Kazakhstan and adjacent Tarim during the Late Permian–Early Triassic. Adopted and modified from Natal'in and Şengör (2005; Tectonophysics, 404, 175–202) with permission from Elsevier Publishing Co. and the authors.

welded together by the Early Permian and moved as a single plate since then (e.g., Zonenshain et al., 1990).

We also need to explain, however, that central South Kazakhstan recorded rotations in a cw as well as ccw sense (Fig. 10), calling for a more complex geometry than a simple sinistral shear zone. While the scale of the displacements along such a shear zone remains unclear, east–west sinistral as well northwest–southeast dextral faults are known to dissect the area. Not all faults (e.g., those shown in Fig. 1) have a known sense of displacement, nor are the ages of the movements that well determined other than for a few faults that were active in post-Permian times, but a conjugate set of strike-slip faults would clearly be capable of producing predominant ccw as well as more localized cw rotations.

Some models have been proposed (e.g., Fig. 12, adopted from Natal'in and Şengör, 2005) that may account for the pattern of rotations, as observed in different parts of Central Asia. Moreover, the fault patterns of this region, its Kazakhstan part in particular, form a dense network, which is variable enough to account for wrench-related rotations. Unfortunately, the sense of noticeable strike-slip displacements is well established for only a few faults; even lower is the number of faults where also the age of displacements can be inferred. To complicate matters further, the sense of strike-slip movements is suggested to have reversed itself at some time in the Permian, as stated in studies of the adjacent Chinese Tien Shan (Wartes et al., 2002, p. 148; Laurent-Charvet et al., 2003, p. 4–20). Also, the Talas–Fergana Fault (TF in Fig. 12) has a dextral displacement of about 200 km (Burtman, 1964) but a large part of the movements happened during the Cenozoic (Thomas et al., 1993). Another major fault in the northeastern part of Kazakhstan, the Chingiz Fault (CH), has a well established dextral displacement of about 100 km (Samygin, 1974), but this motion is also clearly of post-Paleozoic age. In contrast, other major faults, like the Jalair–Naiman Fault (JN) in South Kazakhstan, definitely had dextral displacement (Abdullin et al., 1980), which, however, mostly affected Lower Paleozoic rocks and, to lesser degree, Devonian formations, while evidence for Late Paleozoic motion is ambiguous. Well-dated right-lateral displacements of Late Paleozoic–Early Mesozoic age are well established in the North Tien Shan area near Urumqi (SE part of China's Junggar Basin), but the faults continue into Kazakhstan in a northwesterly direction (Laurent-Charvet et al., 2002, 2003), as can be seen in Fig. 12 (faults TF, JN); this pattern does not necessarily tell us anything about the Kyrgyz–Kazakh parts of the WSW–ENE trending Tien Shan ranges illustrated in Fig. 10 where we infer sinistral shearing. The above examples are not exhaustive, but suffice to show that, despite the large number of faults in Central Asia, their kinematics is so poorly known that at this time we cannot yet fully test the compatibility of structural and paleomagnetic data and that full documentation of the deformation in this area remains elusive.

8. Conclusions

A paleomagnetic study of Upper Paleozoic volcanics and sediments from several localities in southeast Kazakhstan revealed that these rocks retain their prefolding and most probably primary magnetizations. In contrast, several Carboniferous formations carry only postfolding reversed overprints of most likely mid-Permian age, whereas presumably primary Mississippian–Bashkirian components are isolated from just a few sites at two localities. Mean inclinations of both primary and secondary components generally agree with coeval reference directions for Baltica, whereas declinations are deflected counterclockwise in our study area.

The study area belongs to the southern arm of strongly curved Devonian and Late Paleozoic volcanic belts that occupy most of Kazakhstan, and ccw rotated directions are compatible with, but of lesser magnitude than, the rotations inferred from Ordovician–Silurian rocks. Weighing various options for interpreting the rotations in terms of plate tectonic processes, it seems most likely that the Kazakhstan, North Tien Shan and Tarim areas underwent large-scale dextral as well as sinistral wrench-faulting. We speculate that this wrench-faulting was the brittle-crustal response in this area to sinistral oblique convergence between Siberia and Baltica during the Late Permian and Early Triassic, as recently proposed by Natal'in and Şengör (2005). Finally, it is worth noting that such an enormous zone of distributed deformation, manifested as large tectonic rotations, appears to be the largest known so far in the world.

Acknowledgements

We thank Nina Dvorova for paleomagnetic measurements and Alexandra Abrajevitch for critical discussions. Maxim Alexyutin gave permission to cite as yet unpublished results from Middle to Late Paleozoic Kazakhstan rocks. Valerian Bachtadse and Boris Natal'in provided most helpful and constructive reviews that improved the manuscript significantly. This study was supported by the Division of Earth Sciences and the Office of International Science and Engineering's Eastern and Central Europe Program of the U.S.

National Science Foundation, grant EAR 0335882. Support was also derived from the Russian Foundation of Basic Research, grants 04-05-64050 and 05-05-65105, and Program No. 8 of the Earth Science Division, Russian Academy of Sciences.

References

Abdullin, A.A., Volkov, V.M., Scherba, G.N. (Eds.), 1980. The Chu-Ili Ore Belt. Nauka, Alma'ata. 503 pp. (in Russian).

Alexyutin, M.V., Bachtadse, V., Alexeiev, D.V., Nikitina, O.I., 2005a. Paleomagnetism of Ordovician and Silurian rocks from the Chu-Yili and Kendyktas mountains, South Kazakhstan, Geophys. J. Int. 162, 321–331.

Alexyutin, M.V., Alexeiev, D.V., Bachtadse, V., 2005b. Paleomagnetism of Middle and Upper Paleozoic rocks from western and central Kazakhstan. Eos, Trans. - Am. Geophys. Union 86 (52) (Fall Meeting Supplement, abstract GP11A-0004).

Allen, M.B., Şengör, A.M.C., Natal'in, B.A., 1995. Junggar, Turfan and Alakol basins as Late Permian to ?Early Triassic extensional structures in a sinistral shear zone in the Altaid orogenic collage, Central Asia. J. Geol. Soc. (Lond.) 152, 327–338.

Apollonov, M.K., 2000. Geodynamic evolution of Kazakhstan in the early Paleozoic (from the positions of classical plate tectonics). In: Bespaev, K.A. (Ed.), Geodynamics and Minerageny of Kazakhstan, Part 1. VAC Publishing House, Almaty, pp. 46–63. (in Russian)

Audibert, M., Bazhenov, M.L., 1992. Permian paleomagnetism of the North Tien Shan: tectonic implications. Tectonics 11, 1057–1070.

Bai, Y., Chen, G., Sun, Q., Li, Y., Dong, Y., Sun, D., 1987. Paleozoic polar wander path for the Tarim platform and its tectonic significance. Tectonophysics 139, 145–153.

Bazhenov, M.L., Mikolaichuk, A.V., 2004. Structural evolution of Central Asia to the north of Tibet: a synthesis of paleomagnetic and geological data. Geotectonics 38 (5), 379–393.

Bazhenov, M.L., Klishevich, V.L., Tselmovich, V.A., 1995. Paleomagnetism of Permian red beds from south Kazakhstan: DRM inclination error or CRM shallowed directions? Geophys. J. Int. 120, 445–452.

Bazhenov, M.L., Burtman, V.S., Dvorova, A.V., 1999. Permian paleomagnetism of the Tien Shan fold belt, Central Asia: the succession and style of tectonic deformation. Tectonophysics 312, 303–329.

Bazhenov, M.L., Chauvin, A., Audibert, M., Levashova, N.M., 1993. Permian and Triassic paleomagnetism of the south–west Tien Shan: the timing and mode of tectonic rotations. Earth Planet. Sci. Lett. 118, 195–212.

Bazhenov, M.L., Collins, A.Q., Degtyarev, K.E., Levashova, N.M., Mikolaichuk, A.V., Pavlov, V.E., Van der Voo, R., 2003. Paleozoic northward drift of the North Tien Shan (Central Asia) as revealed by Ordovician and Carboniferous paleomagnetism. Tectonophysics 366, 113–141.

Bekzhanov, G.R., Koshkin, V.Y., Nikitchenko, I.I., Skrinnik, L.I., Azizov, T.M., Timush, A.V., 2000. Geological structure of Kazakhstan Academy of Mineral Resources of the Republic of Kazakhstan, Almaty. 394 pp. (in Russian)

Biske, G.S., 1995. Late Paleozoic collision of the Tarim and Kyrgyz–Kazakhstan paleocontinents. Geotectonics 29 (1), 31–39.

Burtman, V.S., 1964. The Talas–Fergana Strike-slip Fault. Nauka, Moscow. 144 pp. (in Russian)

Burtman, V.S., Gurary, G.Z., Belenky, A.V., Ignatiev, A.V., Audibert, M., 1998a. The Turkestan ocean in the Middle Paleozoic: a reconstruction based on paleomagnetic data from the Tien Shan. Geotectonics 32 (1), 15–26.

Burtman, V.S., Gurary, G.Z., Belenky, A.V., Kudasheva, I.A., 1998b. Kazakhstan and the Altai in the Devonian: paleomagnetic evidence. Geotectonics 32 (6), 63–71.

Chuvashov, B.I., 1999. Paleotectonics of the Ural mobile belt and adjacent region in the Late Permian. Doklady Rus. Akad. Sci. 369, 361–364.

Cocks, L.R.M., Torsvik, T.H., 2002. Earth geography from 500 to 400 m.y. ago: a faunal and palaeomagnetic review. J. Geol. Soc. (Lond.) 159, 631–644.

Cogné, J.P., 2003. PaleoMac: a Macintosh application for treating paleomagnetic data and making plate reconstructions. Geochem. Geophys. Geosyst. 4 (1), 1007, doi:10.1029/2001GC000227.

Collins, A.Q., Degtyarev, K.E., Levashova, N.M., Bazhenov, M.L., Van der Voo, R., 2003. Early Paleozoic paleomagnetism of east Kazakhstan: implications for paleolatitudinal drift of tectonic elements within the Ural–Mongol belt. Tectonophysics 377, 229–247.

Degtyarev, K.E., 2003. The position of the Aktau–Junggar microcontinent in the Paleozoides of Central Kazakhstan. Geotectonics 37 (4), 14–34.

Demarest Jr., H.H., 1983. Error analysis for the determination of tectonic rotation from paleomagnetic data. J. Geophys. Res. 88, 4321–4328.

Didenko, A.N., Mossakovsky, A.A., Pechersky, D.M., Ruzhentsev, S.V., Samygin, S.G., Kheraskova, T.N., 1994. Geodynamics of Paleozoic oceans of central Asia. Geol. Geofiz. 35 (7–8), 118–145. (in Russian)

Filippova, I.B., Bush, V.A., Didenko, A.N., 2001. Middle Paleozoic subduction belts: the leading factor in the formation of the Central Asian fold-and-thrust belt. Rus. J. Earth Sci. 3 (6), 405–426.

Fisher, R.A., 1953. Dispersion on a sphere. Proc. R. Soc. London, Ser. A 217, 295–305.

Gilder, S.A., Zhao, X.X., Coe, R.S., Meng, Z., Courtillot, V., Besse, J., 1996. Paleomagnetism and tectonics of the southern Tarim basin, northwest China. J. Geophys. Res. 101, 22,015–22,031.

Gradstein, F.M., Ogg, J.G., 2004. Geologic time scale 2004 — why, how, and where next! Lethaia 37, 175–181.

Grishin, D.V., Pechersky, D.M., Degtyarev, K.E., 1997. Paleomagnetism and reconstruction of Middle Paleozoic structure of Central Kazakhstan. Geotectonics 31 (1), 71–81.

Kirschvink, J.L., 1980. The least-square line and plane and the analysis of palaeomagnetic data. Geophys. J. R. Astron. Soc. 62, 699–718.

Koshkin, V.Y., 1974. Tectonic position of the Balkash–Ili Hercynian volcanic belt. In: Muratov, M.V. (Ed.), Tectonics of the Ural–Mongol Fold Belt. Nauka, Moscow, pp. 85–92. (in Russian)

Kurchavov, A.M., 2001. Geodynamic setting of Devonian continental volcanism of Kazakhstan and southern West Siberia. In: Milanovsky, E.E., Veymarn, A.B., Tevelev, Al. V. (Eds.), Geology of Kazakhstan and the Problems of the Ural–Mongol Fold Belt. Izdatel'stvo Moskovskogo Gosudarstvennogo Universiteta (Moscow State University), Moscow, pp. 65–72. (in Russian)

Laurent-Charvet, S., Charvet, J., Shu, L., Ma, R., Lu, H., 2002. Palaeozoic late collisional strike-slip deformations in Tianshan and Altay, Eastern Xinjiang, NW China. Terra Nova 14 (4), 249–256.

Laurent-Charvet, S., Charvet, J., Monié, P., Shu, L., 2003. Late Paleozoic strike-slip shear zones in eastern central Asia (NW China): new structural and geochronological data. Tectonics 22 (2), doi:10.1029/2001TC901047.

Levashova, N.M., Degtyarev, K.E., Bazhenov, M.L., Collins, A.Q., Van der Voo, R., 2003a. Permian Paleomagnetism of East

Kazakhstan and the amalgamation of Eurasia. Geophys. J. Int. 152, 677–687.

Levashova, N.M., Degtyarev, K.E., Bazhenov, M.L., Collins, A.Q., Van der Voo, R., 2003b. Middle Paleozoic paleomagnetism of east Kazakhstan: post-Middle Devonian rotations in a large-scale orocline in the central Ural–Mongol belt. Tectonophysics 377, 249–268.

Levashova, N.M., Degtyarev, K.E., Van der Voo, R., Bazhenov, M.L., Mikolaichuk, A.V., McCausland, P.J.A., 2005. What did the Uralian Ocean look like? Eos, Trans. - Am. Geophys. Union 86 (52) (Fall Meeting Supplement, abstract GP13B-0004).

Li, Y., McWilliams, M.O., Cox, A.V., Sharps, R., Li, Y., Gao, Z., Zhang, Z., Zhai, Y., 1988. Late Permian paleomagnetic pole from dykes of the Tarim Craton. Geology 16, 275–278.

Mardia, K.V., 1972. Statistics of Directional Data. Academic Press, London. 357 pp.

McFadden, P.L., McElhinny, M.W., 1988. The combined analysis of remagnetization circles and direct observations in paleomagnetism. Earth Planet. Sci. Lett. 87, 161–172.

McFadden, P.L., Reid, A.B., 1982. Analysis of paleomagnetic inclination data. Geophys. J. R. Astron. Soc. 69, 307–319.

McFadden, P.L., Ma, X.H., McElhinny, M.W., Zhang, Z.K., 1988. Permo-Triassic magnetostratigraphy in China: northern Tarim. Earth Planet. Sci. Lett. 87, 152–160.

Natal'in, B.A., Şengör, A.M.C., 2005. Late Palaeozoic to Triassic evolution of the Turan and Scythian platforms: the pre-history of the palaeo-Tethyan closure. Tectonophysics 404, 175–202.

Nie, S.Y., Rowley, D.B., Van der Voo, R., Li, M., 1993. Paleomagnetism of Late Paleozoic rocks in the Tienshan, Northwestern China. Tectonics 12, 568–579.

Samygin, S.G., 1974. The Chingiz Strike-slip Fault and Its Position in the Structure of Central Kazakhstan. Nauka, Moscow. 208 pp. (in Russian)

Şengör, A.M.C., Natal'in, B.A., 1996. Paleotectonics of Asia: fragments of a synthesis. In: Yin, A., Harrison, M. (Eds.), The Tectonic Evolution of Asia. Cambridge University Press, Cambridge, pp. 486–640.

Sharps, R., Li, Y.P., McWilliams, M.O., Li, Y., 1992. Paleomagnetic investigation of Upper Permian sediments in the South Junggar Basin, China. J. Geophys. Res. 97, 1753–1765.

Sharps, R., McWilliams, M.O., Li, Y.P., Cox, A.V., Zhang, Z., Zhai, Y., Gao, Z., Li, Y.A., Li, Q., 1989. Lower Permian paleomagnetism of the Tarim block, northwestern China. Earth Planet. Sci. Lett. 92, 275–291.

Skrinnik, L.I., 1989. The Ketmen series of the North Tien Shan. In: Pushko, E.P., Koshkin, V. Ya. (Eds.), Paleozoic Stratigraphy of Kazakhstan. KazIMS Publications, Alma-Ata, pp. 32–41. (in Russian)

Skrinnik, L.I., 2003. Post-Silurian tectonic evolution of Southeastern Kazakhstan. Geotectonics 37 (3), 65–78.

Skrinnik, L.I., Grishina, T.S., 1997. The stratigraphy of Permian deposits of the Ili mega-synclinorium. Geol. Razved. Nedr Kaz. (Geol. Prospect. Kaz.) (5–6), 8–12. (in Russian)

Skrinnik, L.I., Grishina, T.S., Radchenko, M.I., 1998. The Carboniferous stratigraphy and paleogeography of southeastern Kazakhstan. Geol. Razved. Nedr Kaz. (Geol. Prospect. Kaz.) (4), 9–18. (in Russian)

Tectonics of Kazakhstan, 1982, Explanatory notes to Tectonic map of East Kazakhstan, 1:2,500,000, Nauka, Moscow. 139 pp.

Tevelev, Al. V., 2001. The evolution of the south-eastern margin of the Kazakhstan paleocontinent in the Late Paleozoic. In: Milanovsky, E.E., Veymarn, A.B., Tevelev, Al. V. (Eds.), Geology of Kazakhstan and the Problems of the Ural–Mongol Fold Belt. Izdatel'stvo Moskovskogo Gosudarstvennogo Universiteta (Moscow State University), Moscow, pp. 113–125. (in Russian)

Thomas, J.-Ch., Perroud, H., Cobbold, P.R., Bazhenov, M.L., Burtman, V.S., Chauvin, A., Sadybokasov, E., 1993. A paleomagnetic study of Tertiary formations from the Kyrgyz Tien Shan and its tectonic implications. J. Geophys. Res. 98, 9571–9589.

Torsvik, T.H., Van der Voo, R., Meert, J.G., Mosar, J., Walderhaug, H.J., 2001. Reconstruction of the continents around the North Atlantic at about the 60th parallel. Earth Planet. Sci. Lett. 187, 55–69.

Van der Voo, R., 1993. Paleomagnetism of the Atlantic, Tethys and Iapetus Oceans. Cambridge University Press, Cambridge. 411 pp.

Van der Voo, R., 2004. Paleomagnetism, oroclines and the growth of the continental crust. GSA Today 14 (12), 4–9.

Wartes, M.A., Carroll, A.R., Greene, T.J., 2002. Permian sedimentary record of the Turpan-Hami basin and adjacent regions, northwest China: constraints on post-amalgamation tectonic evolution. Geological Society of America Bulletin 114 (2), 131–152.

Zaytsev, Y.A., 1984. Evolution of Geosynclines: the Oval, Concentrically Zonal Type. Nedra, Moscow. 208 pp. (in Russian)

Zijderveld, J.D.A., 1967. AC demagnetization of rocks: analysis of results. In: Collinson, D.W., Creer, K.M. (Eds.), Methods in Paleomagnetism. Elsevier, Amsterdam, pp. 254–286.

Zonenshain, L.P., Kuzmin, M.I., Natapov, L.M., 1990. Geology of the USSR: a plate-tectonic synthesis. Geodynamics Series, vol. 21. American Geophysical Union, Washington, D.C. 242 pp.